

Corso di Laurea Magistrale in Ingegneria Biomedica

Tesi di Laurea Magistrale

Investigation of the corrosion resistance of a Ti alloy functionalized
with silver nanoparticles.



Relatore:

Silvia Maria Spriano

Candidata:

Francesca Gamna

Corelatori:

Yolanda Hedberg

Martina Cazzola

Sara Ferraris

Inger Odnevall Wallinder

LUGLIO 2019

Summary

Chapter 1	4
1. Introduction	4
Chapter 2	6
2. Body Interaction	6
2.1 Osteointegration.....	6
2.2 Bone Remodeling.....	8
Chapter 3	12
3. Infections	12
3.1 Role of Silver.....	16
3.1.1 Silver Ions.....	17
3.1.2 Silver Nanoparticles	19
3.1.3 Biologic effect of Silver	22
3.1.4 Toxicity of nanoparticles of Silver	24
Chapter 4	26
4. Corrosion of Titanium Alloys.....	28
3.1 Electrochemistry of Ti6Al4V.....	29
3.2 Corrosion behaviour of Ti6Al4V in the body.....	30
3.2.1 Corrosion and proteins	31
3.2.2 Corrosion and implants.....	33
3.3 Corrosion of Titanium functionalized with silver.....	35
Chapter 5	43
5. Materials and methods.....	43
5.1 Samples Preparation.....	43
5.2 Surface Treatment	46
5.3 Surface Characterization	48
5.3.1 SEM.....	48
5.3.2 Profilometry.....	50
5.3.3 Colorimetry.....	52
5.4 Experimental Plan	53
5.4.1 Electrochemical Test	53
5.4.1.1 Setting	53

5.4.1.2 Simulated physiological fluid	56
5.4.1.3 Set Up trouble shouting	57
5.4.1.4 Home made flat cell.....	59
5.4.1.5 Electrochemical test's plan.....	60
5.4.2 Metal Release	61
5.4.2.1 Micro-wave digestion	61
5.4.2.2 Atomic Adsorption Spectroscopy	62
Chapter 6.....	65
6. Results	65
6.1 Surface characterization.....	65
6.1.1 SEM.....	65
6.1.1.1 Cross Section	70
6.1.2 Profilometry.....	72
6.1.3 Colorimetry.....	75
6.1.4 Electrochemical Test	76
6.1.5.1 OCP behaviour	76
6.1.4.2 EIS test	79
6.1.4.3 Potentiodynamic test	83
6.1.5 Metal Release	86
Chapter 7.....	91
7. Conclusions	91

Chapter 1

1. Introduction

Mechanical properties, such as high strength and fracture resistance, long-term and reliable duration give to metallic biomaterials several advantages which make them widely used in the biomedical field. Titanium and its alloys, specifically, are extensively used in applications such as dentistry, orthopaedic devices and bone fixation systems. Ti-6Al-4V is the principal titanium alloy used in implants, it is an alpha-beta alloy containing 6% of aluminium which is an alpha phase stabilizer and 4% vanadium which is a beta phase stabilizer. Its high employment is due to good mechanical properties, high flexibility and strength, biocompatibility, and corrosion resistance [1]. Despite the high corrosion resistance of the material, implant failures due to corrosion problems are possible to find in medical literature [2]. Since physiological liquid is not a relative aggressive environment for an implanted metal alloy, corrosion represents a concern in the biomedical field, as it leads to the release of ions and particles in peri-implant tissue which may result in inflammation, material degradation, and even necessary extraction of the prosthesis.

In addition to corrosion, bacterial infections represent another critical factor which could affect the success of the implant. Prosthetic infections constitute a complication which is not frequent, but potentially devastating of the joint prosthesis implants. Normally, infections are locally treated with antibiotics, even if they cannot guarantee an effective solution. That's why there is an interest in biomedical research to focus on finding a way to inhibit infection and biofilm formation with alternative

antibacterial solutions. The use of silver as an alternative solution has been taken into consideration, as it ensures antimicrobial properties able to avoid infections. It could however also influence the good corrosion resistance of titanium in a negative way, by galvanic coupling. Therefore, the focus of this thesis is the investigation of the corrosion behaviour and release of metal ions of these implant materials, using samples on Ti6Al4V alloy treated superficially and functionalized with nanoparticles of silver.

Chapter 2

2. Body-interaction

Implants are initially osseointegrated through various phases involving inflammation and bone remodeling coordinated by the action of osteoclasts and osteoblasts. Over time, even well-integrated prostheses may suffer from infection and the creation of a superficial bacterial biofilm. The steps of this interaction will be explored in this chapter.

2.1. Osseointegration

Osseointegration is defined as a real and direct contact between the implant and the bone without the presence of fibrous tissue. This means that, if the osseointegration works well, the bone should be firmly anchored to the implant without growth of other tissue at the interface. The definition of osseointegration was coined in 1950s by professor Per-Ingvar Branemarg who showed that metallic titanium could be permanently incorporated into the bone [3]. It is therefore easy to see that osseointegration is an important key for the success of an implant.

Underlying osseointegration is bone formation characterized by osteocyte formation from osteoblasts, so from undifferentiated mesenchymal cells (Figure 1.1).

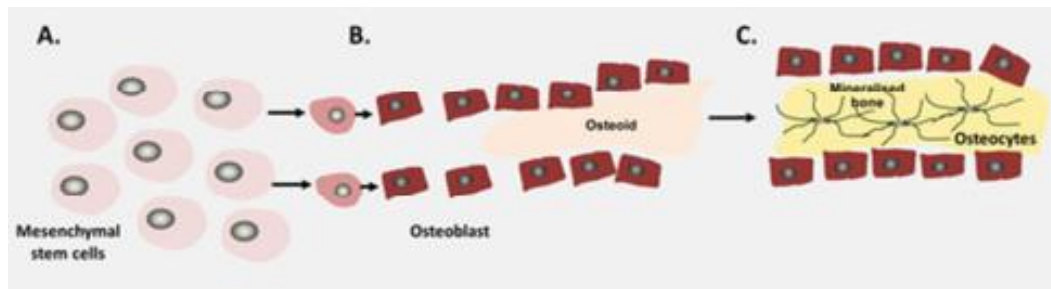


Figure 1.1 Diagram illustrating bone formation starting with Mesenchymal Stem Cell [8]

The osseointegration process involves several linked events such as protein adsorption, coagulation of blood followed by the recognition of the surface by mesenchymal stem cells and finally, if the surface is suitable, bone formation through their differentiation into bone cells. The first interaction concerns the adhesion of proteins of blood on the surface followed by the interaction with blood cells, including red cells and platelets responsible of the clot and the fibrin matrix formation which is fundamental for the migration of osteogenic cells.

Many different factors influence the process of osseointegration which include the type of material and its biocompatibility, the implant surface, its chemical composition and topography, as the protein adsorption is strongly influenced by surface properties [17],[18].

As said in the introduction, among the various materials for implants, titanium and its alloys are frequently used, mostly in the dental implants, and one of the reasons of that is precisely their high osseointegrability, and high biocompatibility.

Acting on the surface we can facilitate osseointegration by making the osteoinductive or bioactive material, thus stimulating the differentiation of osteoblasts. Modifications

of the surface such as sand blasting, acid etching or heat treatment create a micro - submicro roughness which enhances the osseointegration.(Figure 1.2)

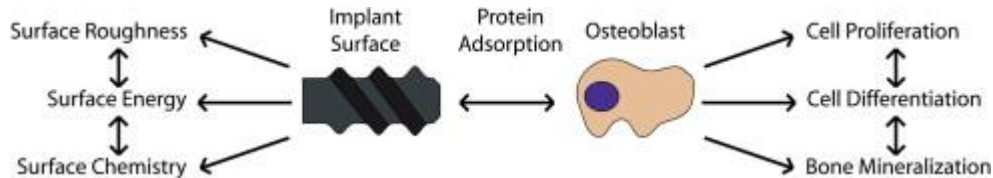


Figure 1.2 Interaction between superficial properties of the implant and biological consequences [18]

2.2. Bone remodeling

In addition to osseointegration as a key factor, there is definitely the process of bone remodeling that is established around the osteointegrated implant [4]. In fact, the bone damaged for implant preparation has osteocytic lacunas that remain even after osseointegration and which can only be filled thanks to bone remodeling [5].

Bone remodeling is a fundamental renewal process balanced by bone resorption followed by bone formation and a good performance of this is essential for implant success [6]. The protagonists of these two processes are osteoclasts and osteoblasts, respectively. In brief, through bone resorption, osteoclasts destroy old bone and through bone formation osteoblasts create new bone that will subsequently mineralize. In particular, bone remodeling is composed by 5 overlapping steps of activation, resorption, reversal, formation and termination [6] (Figure 1.3).

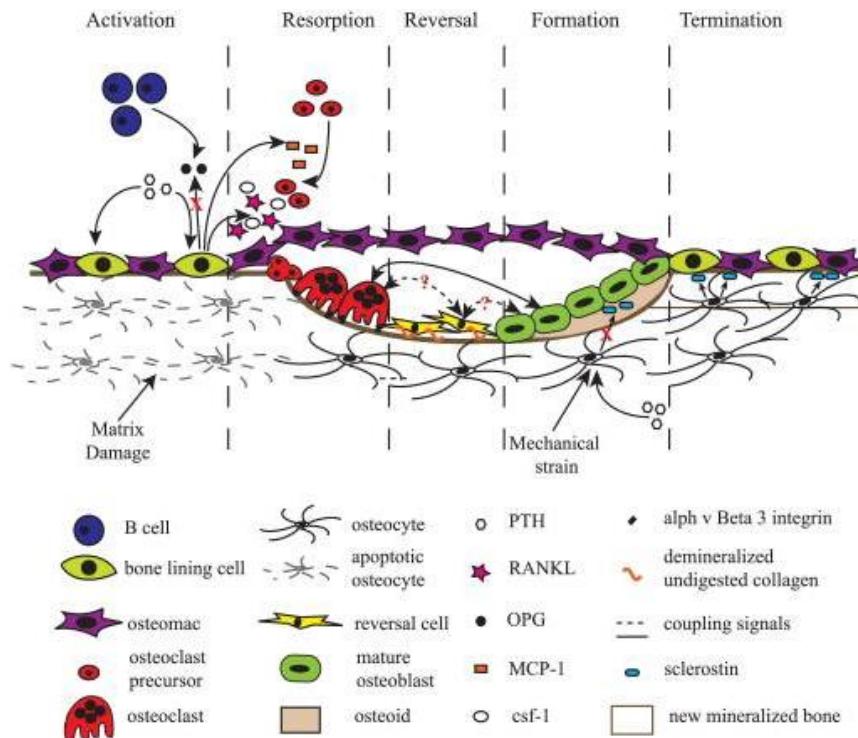


Figure 1.3 Schematic representation of bone remodeling [11]

Since osteoclasts dictate the development of bone resorption, they are responsible of a group of disorders characterised by bone loss. Furthermore, their activity plays a very important role at the bone-biomaterial interface throughout the period of the implant as it prepares the surface at the interface for osteoblast activity and allows bone remodeling reinforcing its internal structure along the mechanical loading lines [7].

Going more specifically, osteoclasts differentiation requires stimulation by RANKL which is a cytokine secrete by osteoblasts if stimulated by the parathormone PTH. Osteoblasts, in addition to producing cytokines that favour osteoclastogenesis, secrete OPG, other cytokine also known as osteoclastogenesis inhibitory factor which binds with RANKL decreasing the number of ligands that activate the osteoclasts. The process of this regulation is explained in Figure 1.4.

In light of this, it is easy to affirm that osteoclastogenic and anti-osteoclastogenic cytokines play a key role in bone remodeling and a dysregulation of this balance can lead bone disease or abnormalities [15].

In this regard, Palmqvist et al [57], in one of their works, have proven the importance of some cytokines such as IL-4 and IL-13 in inhibiting bone resorption stimulated by other cytokines such as RANKL and TNF- α . This inhibitory effect is thought to involve decreased osteoclastogenesis, as they saw in their experiment that the presence of IL-4 and IL-13 inhibited the formation of osteoclasts in mouse bone marrow cultures. By gene expression testing during osteoclastogenesis, they noted a decrease in mRNA expression of proteins encoding for RANKL, resulting in a decrease in differentiation into osteoclasts (Figure 1.5).

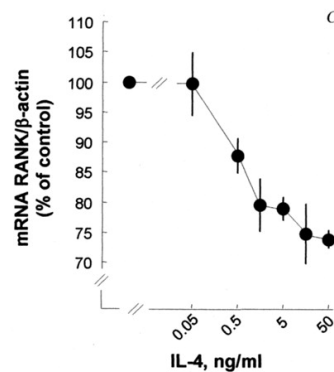


Figure 1.5 Effect of IL-4 in RANK expression [57]

On the other hand, in osteoblasts, both an increase in mRNA RANKL and a decrease in mRNA OPG and in the proteins produced by vitamin D3 have been observed and reversed by the presence of the two cytokines IL-4 and IL-13. and IL-13 (Figure 1.5).

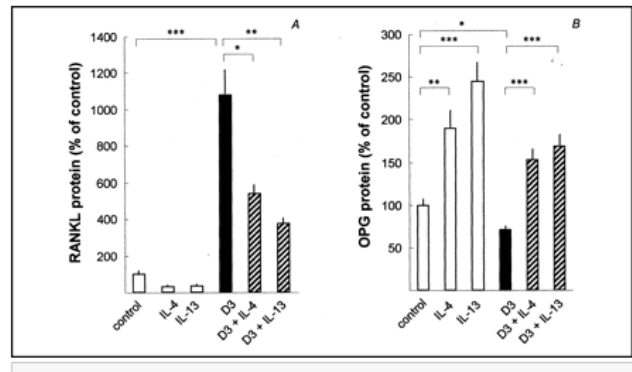


Figure 1.6 Inhibition of vitamin D3-stimulated RANKL protein expression and contrast of D3-induced OPG decrease in mouse bones [57]

Chapter 3

3. Infections

The estimated annual incidence of infection is around 2% and 1% for hip, knee and shoulder replacements, respectively, interestingly for both younger and older adult patients. The most common infection is caused by staphylococcus aureus and epidermidis, which are gram-positive bacteria and in the case of titanium implants, *S. epidermidis* is the bacteria which mainly adheres on the surface [3], [22]. There are many factors that influence the initial attachment of bacteria to the foreign surface and the subsequent development of biofilm, for example, the creation of biofilm occurs more frequently in surfaces that are more rough and more hydrophobic and where there is a high concentration of protein adsorbed. In Table 1, it is shown which are the most important factors that influence the bacterial attachment and the biofilm formation.

Table 1.1 Variables that favour the growth of biofilm [23]

Adhesion surface	Bulk fluid	Cell
Texture or roughness	Flow velocity	Cell surface hydrophobicity
Hydrophobicity	pH	Extracellular appendages
Surface chemistry	Temperature	Extracellular polymeric substances
Charge	Cations	Signalling molecules
Conditioning film	Presence of antimicrobial products	
	Nutrient availability	

Biofilm formation is the result of a system of cooperation and coordination of gene expression among bacterial cells and could be explained in four steps:

1. Deposition and adsorption of a single bacterial cell on the foreign surface
2. Aggregation of more bacterial cells and their growth, starting to create a biofilm
3. Maturation of a biofilm
4. Detachment of a part of the colony which start to spread into the surrounding.

(Figure 1.5)

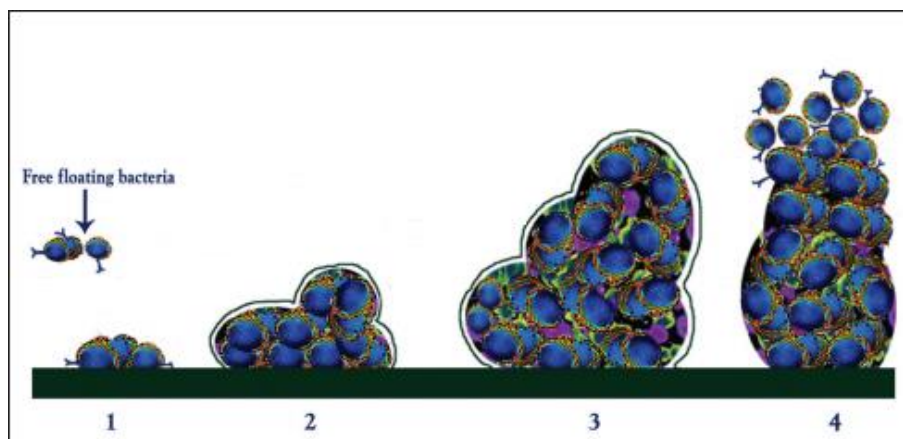


Figure 1.5 Scheme of biofilm formation [22]

The formed biofilm is composed by 15% of bacterias and the rest is composed by the matrix material, known as EPS (extracellular polymeric substances).

The components involved consist mainly of proteins, DNA and polysaccharides and they form the scaffold of the biofilm ensuring cohesion and adhesion on the surface. Moreover, EPS works as glue among cells, allowing communication between them, guarantees protection and provides nutrients [25]. In Table 1.2, it is shown which are the substances that make the EPS and their relatively functions.

The usual therapy to fight biofilm formation is the treatment with antibiotics which are able to affect the infection, but not to eliminate the cause. Moreover, biofilm develops resistance against drugs which means that they have no effect on infection [22].

The resistance mechanism is not yet fully known, but it is clear that biofilm should has some intrinsic properties which allow high resistance to the conventional antibiotics such as (a) biofilm's structure, which interferes with the drug diffusion, (b) slow growth of biofilm, which causes antibiotics to be taken slowly and this gives time to infection to spread. (c) Biofilm's phenotype, which is considered as a group of bacterial cells that is not affected by antibiotics [24]

Table 1.2 Functions of substances in the biofilm [25]

Function	Relevance for biofilms	EPS components involved
Adhesion	Allows the initial steps in the colonization of abiotic and biotic surfaces by planktonic cells, and the long-term attachment of whole biofilms to surfaces	Polysaccharides, proteins, DNA and amphiphilic molecules
Aggregation of bacterial cells	Enables bridging between cells, the temporary immobilization of bacterial populations, the development of high cell densities and cell-cell recognition	Polysaccharides, proteins and DNA
Cohesion of biofilms	Forms a hydrated polymer network (the biofilm matrix), mediating the mechanical stability of biofilms (often in conjunction with multivalent cations) and, through the EPS structure (capsule, slime or sheath), determining biofilm architecture, as well as allowing cell-cell communication	Neutral and charged polysaccharides, proteins (such as amyloids and lectins), and DNA
Retention of water	Maintains a highly hydrated microenvironment around biofilm organisms, leading to their tolerance of desiccation in water-deficient environments	Hydrophilic polysaccharides and, possibly, proteins
Protective barrier	Confers resistance to nonspecific and specific host defences during infection, and confers tolerance to various antimicrobial agents (for example, disinfectants and antibiotics), as well as protecting cyanobacterial nitrogenase from the harmful effects of oxygen and protecting against some grazing protozoa	Polysaccharides and proteins
Sorption of organic compounds	Allows the accumulation of nutrients from the environment and the sorption of xenobiotics (thus contributing to environmental detoxification)	Charged or hydrophobic polysaccharides and proteins
Sorption of inorganic ions	Promotes polysaccharide gel formation, ion exchange, mineral formation and the accumulation of toxic metal ions (thus contributing to environmental detoxification)	Charged polysaccharides and proteins, including inorganic substituents such as phosphate and sulphate
Enzymatic activity	Enables the digestion of exogenous macromolecules for nutrient acquisition and the degradation of structural EPS, allowing the release of cells from biofilms	Proteins
Nutrient source	Provides a source of carbon-, nitrogen- and phosphorus-containing compounds for utilization by the biofilm community	Potentially all EPS components
Exchange of genetic information	Facilitates horizontal gene transfer between biofilm cells	DNA
Electron donor or acceptor	Permits redox activity in the biofilm matrix	Proteins (for example, those forming pili and nanowires) and, possibly, humic substances
Export of cell components	Releases cellular material as a result of metabolic turnover	Membrane vesicles containing nucleic acids, enzymes, lipopolysaccharides and phospholipids
Sink for excess energy	Stores excess carbon under unbalanced carbon to nitrogen ratios	Polysaccharides
Binding of enzymes	Results in the accumulation, retention and stabilization of enzymes through their interaction with polysaccharides	Polysaccharides and enzymes

To cope with the problem of resistance, many antibacterial methods have been designed. Knowing the factors that influence bacterial adhesion, strategies have been studied to avoid bacterial contamination without the use of antibiotics.

In the next paragraphs, a method that uses silver nanoparticles as an antibacterial agent.

3.1. Role of Silver

Historically, several metals including arsenic, mercury and silver have proven effectiveness in treatment of infections in humans. These metals inhibit the growth of a broad spectrum of bacteria at very low concentrations. Especially silver is widely used in the pharmaceutical industry and in many consumer products. Silver products have two fundamental advantages: have good and broad-spectrum antimicrobial activity and no associated bacterial resistance has been developed.

Silver as an antibacterial agent can be found in different forms: silver sulfadiazine, silver nitrate and silver nanoparticles. The first two cases are composed by silver ions dissolved in a solution, which represent the protagonists of the antibacterial action. The case of silver nanoparticles is quite different, in which the mechanism of action is based on the destruction of bacteria caused by the particles themselves.

Nanoparticles of silver (AgNP) have gained a considerable attention, with the recent development of nanotechnologies, since their good antibacterial activity against Gram-Positive as well as Gram-Negative bacteria. Particle size plays an important role in the antimicrobial effect, related to the higher surface/volume ratio which brings an higher amount of ions release. The nanometric dimensions give also the possibility to use less expensive materials and to have greater efficiency [26].

The modes of action of silver ions (Ag^+) is strictly linked to the ions concentration of the solution, furthermore, it has been proven that the ionic action is very similar and even stronger to that of the nanoparticles, probably due to the life cycle of silver nanoparticles and their transformation to silver ions [28].

In fact, in both cases, one of the most important *modus operandi* is based on the increase in ROS production which corresponds to an increase in the concentration of

H₂O₂. This fact leads to an oxidative imbalance inside the bacteria which causes a proliferative inhibition.

To reach this state, silver, in whatever form it is, must be able to enter through the bacterial membrane. The interaction of silver and the cell wall is one of the most important mechanisms for its toxicity and represents the point of attack for the antimicrobial activity [26].

3.1.1. Silver Ions

The antibacterial mechanism of silver ions is based on interactions with different biomolecules that are found within the bacterial cell, such as nucleic acids, in the bacterial membrane and in the key functional groups of metabolic enzymes [41].

Silver ions form bonds mainly with sulphur, oxygen and nitrogen. For this reason, Ag⁺ is able to create bonds with metabolic enzymes and proteins with S-pending groups and with nitrogen groups characteristic of the DNA chain [42]. For these reasons, a mechanism is also active within our organism that has the effect of reducing the toxicity of silver ions, as all sulphur-containing human cell components, such as glutathione and cysteine, can bind with silver and render it inactive [41]. The interaction of Ag⁺ with thiol groups is one of the most important incisive mechanisms in the antimicrobial role of silver, also considering other groups present in cellular components, such as hydrogen binding, that may be involved in the interaction with silver [39].

As a result of everything that is just been said, silver ions can interfere with the metabolism of the bacterial cell by:

- Interaction with nucleic acids, with the consequence of an inhibition of the replication and condensation of DNA
- Increase in the production of ROS, caused by the inhibition of the main respiratory chain proteins with a consequent oxidative stress.
- Bonds with the enzymes or proteins, especially those with thiol groups.
- Bonds with S2 protein, localized in small subunits of the bacterial ribosome.

Moreover, it should be considered that, silver ions cause the release of K ions from the bacteria, which is why cytoplasmic membrane is an important target for silver ions [39][26]. The diagram below (Figure 2.1) shows the mechanism of action of silver ions on bacteria

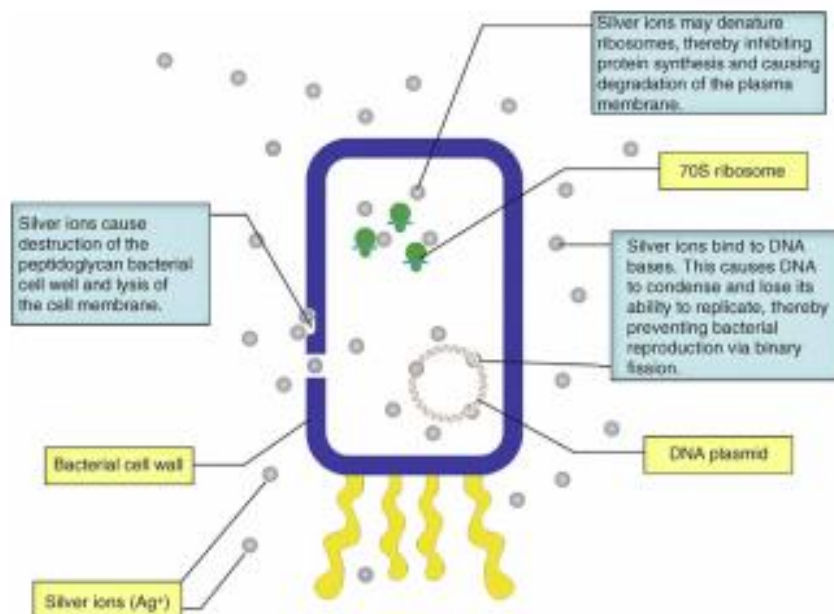


Figure 2.1 Scheme that represents interaction of silver ions with bacteria [42]

3.1.2. Silver Nanoparticles

Nanoparticles of silver can be found either dispersed in solution, the colloidal solutions, or stabilized and functionalized on surfaces. Since the colloidal solutions represent a relatively low stability for nanoparticles which tend to aggregate, the usage of stabilized AgNPs has been proposed. This fact allows to obtain particles which, being stabilized, have a greater activity and effectiveness [38].

Nanoparticles of silver, once in contact with biological aqueous solution, are able either to release in the surrounding environment Ag^+ ions by an oxidative process, undergoing a superficial oxidation or interact with biological macromolecules [37][40] (Figure 2.2).

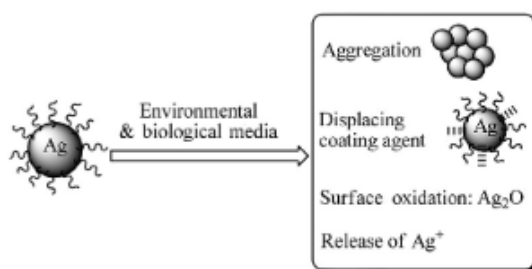


Figure 2.2 Scheme that represents interaction of silver nanoparticles in the biological environment [40]

In general, the antibacterial activity of AgNPs is dependent on particle size as it represents an incisive factor for the ion release.

In fact, small nanoparticles with a diameter around 10 nm are more consistent in the ion release and, consequently, the bactericidal effect is dominated by Ag^+ ions interactions. Because of that, it is sometimes difficult to distinguish the two mechanisms of action specific to ions and AgNPs.

The interaction between AgNPs and the bacteria is mainly due to the crossing of the bacterial membrane that allows silver to meddle in the bacteria's metabolism. Once

inside, AgNPs could interfere with bacterial DNA or stimulate ROS production in the cytoplasm. In the other hand, the accumulation of nanoparticles in the cell could lead to the lysis of the cell itself and therefore to its death [28]. In the figure below (Figure 2.2), it is shown the schematic representation of the AgNPs mechanism of action on the bacterial biofilm.

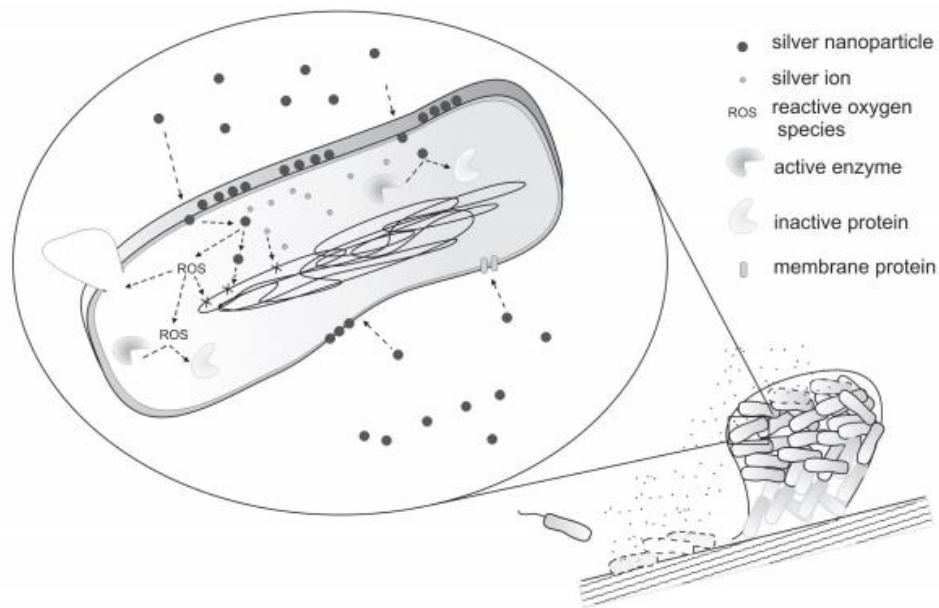


Figure 2.3 Scheme that represents the modus operandi of nanoparticles of silver on the biofilm [38]

A complete comparison between the mode of action of silver ions and silver nanoparticles against the two types of bacteria (Gram-positive and Gram-negative), with a brief description, is presented in the figure below (Figure2.4).

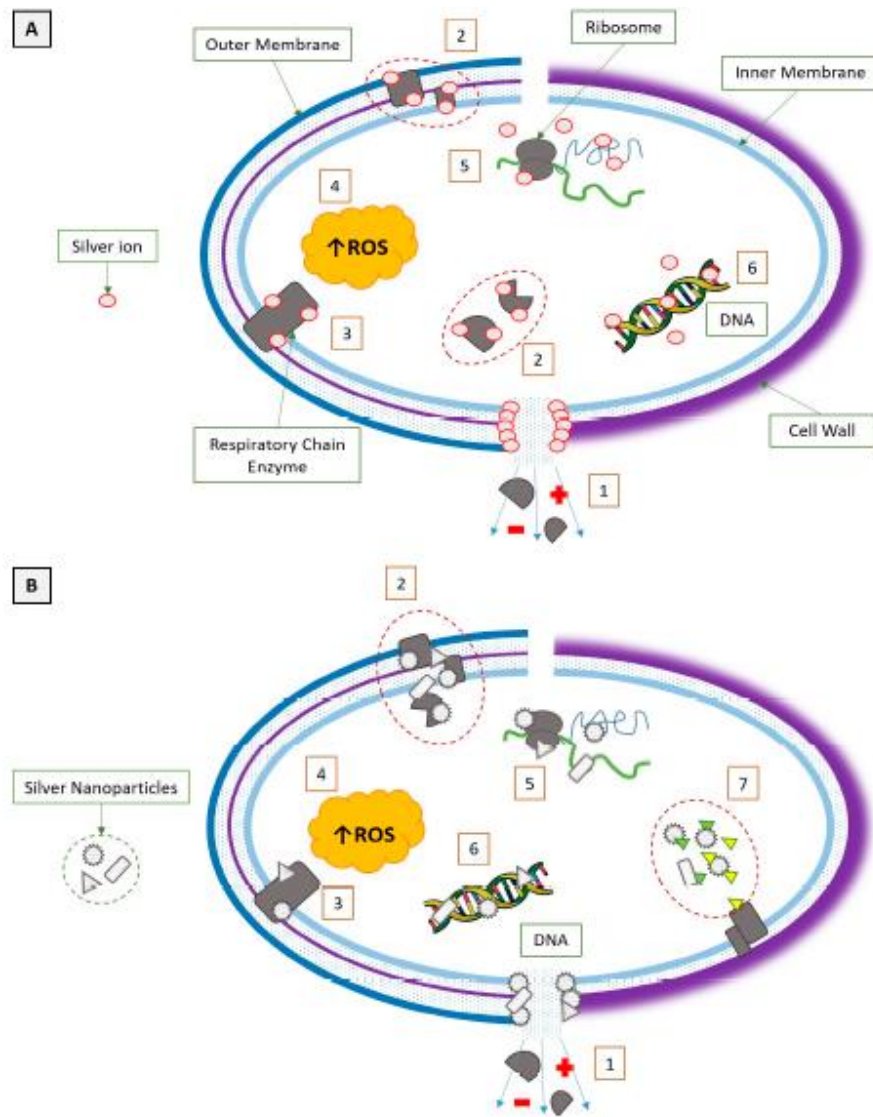


Figure 2.4 A comparison between mode of action of the silver ions and silver nanoparticles to and Gram-positive (**right**) and Gram-negative (**left**) bacteria. (1) Pore formation with ion loss (2) Denaturation of cytoplasmic proteins and enzymes (3) Inactivation of respiratory chain enzymes (4) Increase of ROS concentration (5) Interaction with ribosome (6) Interaction with nucleic acids of DNA (7) Inhibition of signal transduction

3.1.3. Biologic effect of Silver

In the first chapter it was explained how the bone remodeling was an important factor for the success of an implant. At the base of bone remodeling, there is the communication of hormones and signal factors like cytokines, which modulate the balance between osteoclastogenesis and osteoblastogenesis. We remember that cytokines play a key role in the modulation of immune system and they are classified into two types, proinflammatory, that induce osteoclastogenesis and anti-inflammatory that induce osteoblastogenesis. Having said that, it is important to understand the mechanism and the potential effect of the silver nanoparticles on the production of cytokines and their impact on bone cells. As already mentioned, the broad-spectrum, and high antimicrobial effect, has greatly increased the interest on the use of nanosilver as antibacterial agent. Despite this, there is still a lack of knowledge concerning the effect of the silver on bone remodeling mechanism [29].

In general, an imbalance between pro-inflammatory and anti-inflammatory cytokines can lead to increased susceptibility to infection, which can also be promoted by the presence of AgNPs. According to this theory, it had been proven that a non-toxic dose of AgNPs ($\leq 1 \mu\text{g/ml}$) inhibit the mRNA expression levels of cytokines, in particular of the tumor necrosis factor (TNF- α), which is a proinflammatory cytokine [31]. It is well known that the induction of TNF- α can lead to cellular apoptosis which suggests that the inhibitory effect of AgNPs on TNF- α could have an anti-apoptotic effect and it might inhibit inflammations associated to infections. On the other hand, it is interesting to note that the inhibition of TNF- α can also have effects on cellular

responses and activities that can lead to reduce cellular survival. Therefore, whether through inhibition or induction of TNF- α , cell survival is reduced [32],[33]. AgNPs might have also beneficial effect on bone formation as they could promote the proliferation and osteogenesis of mesenchymal stem cells (MSC) [34]. In contradiction to the above, a work of Hongjun Xie et al. suggests that AgNPs may interfere with bone formation and it recommends to have more attention to the potential toxicity of AgNPs during the design of orthopaedic implants [36]. Among all the papers, it is easy to find different opinions regarding the effect of nanoparticles on bone cells but in general, we can say that:

- AgNPs have an inhibition effect on the production of cytokine TNF- α , resulting in an inhibition of osteoclastogenesis and inflammation.
- It is important to consider the concentration of AgNPs, aware that a low dose of AgNPs might promote bone formation, but a wrong concentration can also lead to an opposite effect.

3.1.4. Toxicity of nanoparticles of silver

Nanoparticles have been shown to have a toxicity effect both at a general level for humans and at a cellular level with the risk of inducing genotoxicity and cytotoxicity [43],[44]. Tianlu Zhang et al, in one of their works, they injected AgNPs through the tail into a male mouse and traced the pathway demonstrating that factors such as size, chemical surface, exposure method are critical for determining their tissue distribution and relative toxicity. They also found that lungs, liver and kidneys were the first target organs after injection, and in particular, they detected that distribution to the lungs and liver induced cell infiltration and alveolar inflammation [43].

At the cellular level, cell uptake can occur either through the interaction with membrane proteins which activates signalling pathways or by diffusion or endocytosis. Nano-silver uptake corresponds to the formation of ROS, caused by the interaction with the mitochondria and its consequent dysfunction [40]. In terms of genotoxicity, once inside, AgNPs can cause damage to nucleic acids by increasing ROS production or by decreasing ATP production, thereby hindering the DNA repair mechanism that is ATP-dependent [45]. In the figure below it is proposed a mechanism of nanosilver cytotoxicity (Figure 2.5).

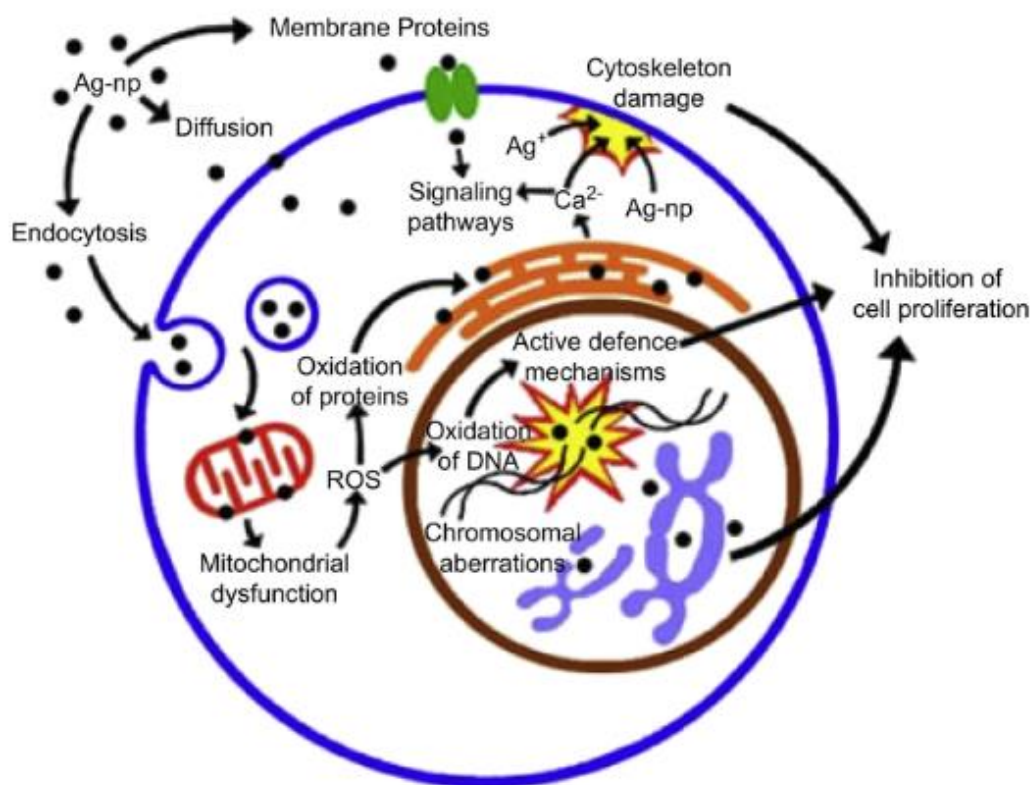


Figure 2.5 Mechanism of nanosilver cytotoxicity [40]

Chapter 4

4. Corrosion of titanium alloys

One of the reasons why titanium alloys are very often used in biomedical applications is because they have very good corrosion resistance. Titanium alloys, as soon as they are exposed to water or air, form a passive, adherent layer of titanium oxide caused by the reaction between titanium and oxygen. The oxide layer usually forms very quickly in a few seconds reaching thickness of few nanometers and, being a chemically very stable film ($\Delta G = -889.5 \text{ kJ mol}^{-1}$), it makes titanium very resistant to corrosion and chemically, thermally stable and that can only be attacked by a few substances such as hydrofluoric acid [46][47][51]. Typically in titanium alloys, metals such as Al, V, Mo, Nb are added to try to increase the passive state. Of all, the Ti6Al4V with ($\alpha+\beta$) structure was chosen as the alloy with greater resistance to corrosion in a saline environment [48].

The oxide film consists of titanium dioxide (TiO_2), which may be amorphous or crystalline depending on the growth conditions [49]. TiO_2 is an important photocatalytic material that exists as two main polymorphs, anatase and rutile. The differences between anatase and rutile and their properties are presented in the table below [50].

Table 3.1 Property of anatase and rutile [50]

Property	Anatase	Rutile
Crystal structure	Tetragonal	Tetragonal
Atoms per unit cell (Z)	4	2
Space group	$I_4^1A_2md$	P_4^2Am
Lattice parameters (nm)	$a = 0.3785$ $c = 0.9514$	$a = 0.4594$ $c = 0.29589$
Unit cell volume (nm ³) ^a	0.1363	0.0624
Density (kg m ⁻³)	3894	4250
Calculated indirect band gap		
(eV)	3.23–3.59	3.02–3.24
(nm)	345.4–383.9	382.7–410.1
Experimental band gap		
(eV)	~ 3.2	~ 3.0
(nm)	~ 387	~ 413
Refractive index	2.54, 2.49	2.79, 2.903
Solubility in HF	Soluble	Insoluble
Solubility in H ₂ O	Insoluble	Insoluble
Hardness (Mohs)	5.5–6	6–6.5
Bulk modulus (GPa)	183	206

4.1. Electrochemistry of Ti6Al4V corrosion

Ti6Al4V is a passive metal that has active behaviour at very low potentials.

Figure 3.1 shows a schematic polarisation curve of a generic passive metal that shows [49]:

- E_{pp} (primary passivation potential): point of potential before which the corrosion/dissolution ratio tends to increase (active region) and beyond which it tends to decrease
- I_{crit} (critical anodic current density): current density at the potential E_{pp} which represents the highest dissolution rate.
- I_{pass} (passive current density): current density that does not change significantly and it occurs when potential is higher than E_{pp} (passive region).

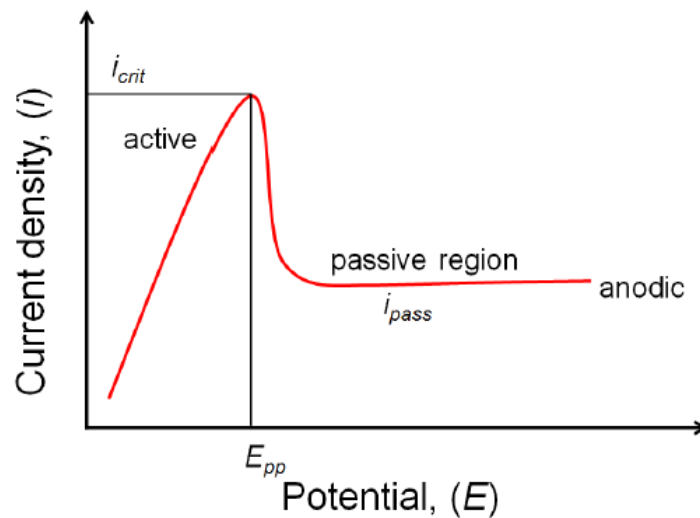


Figure 3.1 Polarisation curve of a generic passive metal [49]

The corrosion of the metal can be evaluated by means of electrochemical tests and by analysing the polarization curves which will be explained in detail in the following chapter.

In general, the cathodic reaction is the reaction dictated by the environment and the electrolyte, when its rate is low then E_{corr} is in the active zone. When it is very high, E_{corr} is in the passive zone (Figure 3.2) [49].

This last case is the case of metals such as Pd to Ti (and its alloy) in which the oxide layer protects them from corrosion.

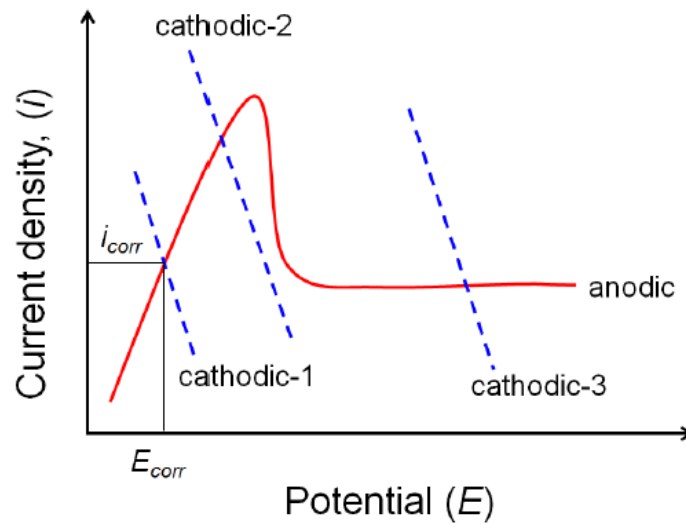


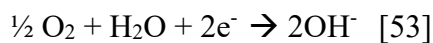
Figure 3.2 Polarisation curve with cathodic reaction [49]

4.2. Ti6Al4V corrosion behaviour in the body

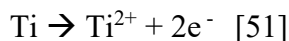
As already pointed out, the titanium alloys have a very good resistance to corrosion, despite this, titanium implants in contact with biological fluids may behave unexpectedly. As is well known, the biological fluid is a saline solution with a slightly basic pH. In particular, the peri-implant environment contains biological species such as albumin and hydrogen peroxide, which can alter corrosive behaviour [52]. Corrosive dissolution is considered one of the most important mechanism for the introduction of foreign ions in the body which can cause a clinically significant problem. This interaction can lead either to implant failure to function, have a negative effect on the patient resulting in implant rejection from surrounding tissue or infections such as metallosis, or both.

Various corrosion studies in different media that imitated physiological solution were made to calculate the rate and corrosion resistance of the metal alloy.

In general in a basic environment like the physiological one, the cathodic reaction is determined by the following equation:



While the anodic region is determined by the following equation:



Human body is a very corrosive environment also because it is a combination of corrosion types influenced by fretting, salts, and geometry of implants.

4.2.1. Corrosion and proteins

When the implant comes into contact with the body, one of the first things that happens is the adsorption of proteins on the foreign surface. This fact is important to consider in the study of corrosion as adsorption can influence the degradation of the metal [53]:

- It could create a coating on the surface and inhibit the cathodic reaction [54]
- It mediates the cell adsorption
- It can act as a lubricant

Moreover, proteins like albumin could create a bond with superficial metal and, if the complex metal-albumin is stronger than the complex metal-oxide, it could provoke the detachment of the metal and increase the degradation rate. The figure below presents an illustration of the effect of proteins on metal degradation.

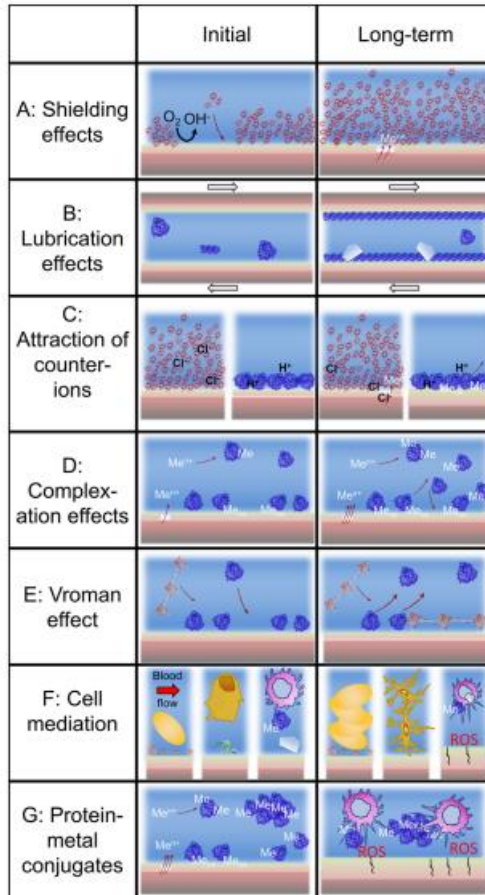


Figure 3.2 Illustrations of different mechanisms of protein-induced or -inhibited corrosion of a passive metal

[54]

4.2.2. Corrosion and implants

As already mentioned, titanium-aluminium-vanadium alloys have shown excellent resistance to corrosion, but are subject to friction and wear. A current problem with orthopaedic alloys is the corrosion of the connections most affected by shear forces, i.e. the conical connections at the points of the spare parts. The higher the number of joints in a prosthesis that include conical connections between metal and metal, the more important the effect of cracks, stresses and movements become. The interaction between the implant and the tissue can lead to the release of metallic ions from the implant. The figure 3.3 explains the cell adhesion that occurs on the interface, once that the implant comes into contact with the tissue. Cell adhesion also affects a whole range of proteins and biomolecules such as proteins adhesion on the surface layer of the metal. The cell adhesion could have some effect on the release of the metallic ions. Specifically, the presence of the cell on the surface could have two different effects:

1. Decrease of the cathodic reaction, due to the layer composed of cells which decrease the O_2 quantity on the interface.
2. Dissolution of the metal ions in vicinity to the cell with the accumulation of Cl^- , could lead to a decrease of the protectiveness of the passive film.

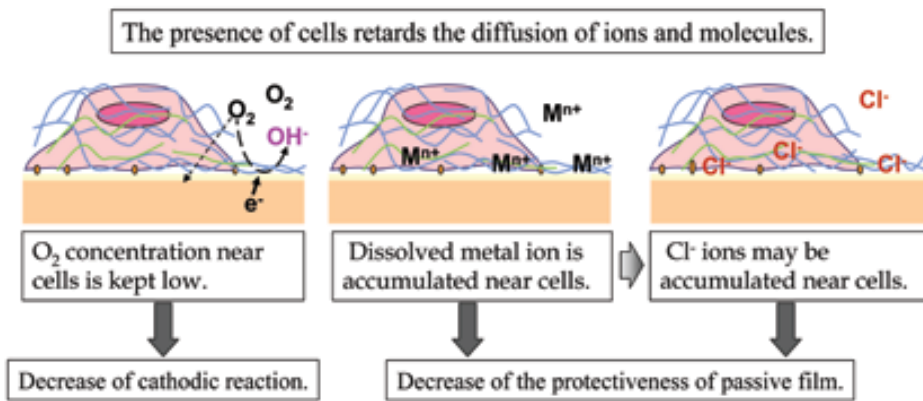
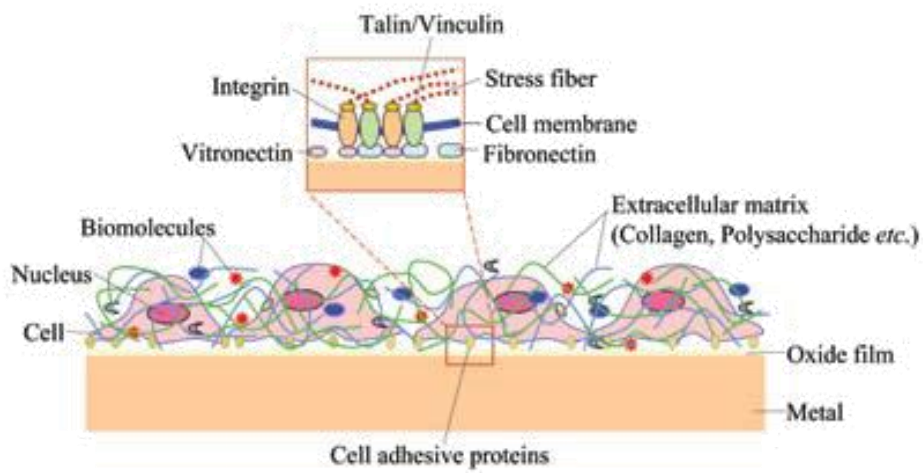


Figure 3.3 Cell adhesion and its effect on the oxide film [ref]

4.3. Corrosion of titanium functionalized with silver

Implant surface is usually treated to increase osseointegration. Functionalisation with nanoparticles is carried out to make the surface biocompatible, bioactive or antibacterial. However, it is important to understand whether the treatments have an impact on the level of corrosion, even if corrosion of biomedical metallic materials is inevitable.

Guisen Wang, Yi Wan et al. [55] studied the corrosion behaviour in different groups of samples (smooth, microstructured, micro-nanostructured and functionalized with nanoparticles of silver), through electrochemical tests in Ringer's solution (which consisted of 8.6g NaCl, 0.3g KCl, 0.33g CaCl₂ in 1L of distilled water). They analysed the polarisation curve to discover the corrosion resistance of each group of samples. The results indicated that the sample functionalized was the one with the higher corrosion resistance and, in general, the surface morphology is an important factor that improve the corrosion resistance (Figure 4.4).

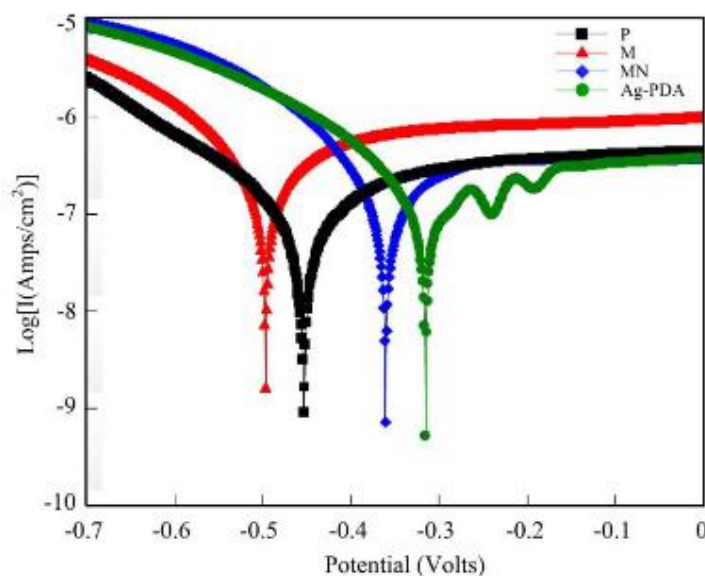


Figure 4.4 Polarisation curves of the four groups of samples [55]

Another work [56], which is based on the functionalization with nanoparticles of zinc (ZnO), discovered that the incorporation of ZnO nanoparticles into the coatings resulted in reduction in the number of pores, and modification of the coating microstructure, which consequently increased the corrosion resistance, along with a reduction of corrosion current density.

References:

- [1] Xuanyong Liu, Paul K. Chu, C.X. Ding
“Surface modification of titanium, titanium alloys, and related materials for biomedical applications” *Materials Science and Engineering: R: Reports, Volume 47, Issues 3–4, Pages 49-121, 2004*
- [2] P. Hallam, F. Haddad, J. Cobb “Pain in the well-fixed, aseptic titanium hip replacement *THE ROLE OF CORROSION*”, *J Bone Joint Surg [Br], Volume 86(B), Pages 27-30, 2004.*
- [3] Rajeshwari Nair, PhD, MBBSa,b , Marin L. Schweizer, PhDa,b, *, Namrata Singh, MD, MSCIA,b, “Septic Arthritis and Prosthetic Joint Infections in Older Adults”, *Infect Dis Clin N Am, Volume 3, Pages 715–729, 2017.*
- [4] Rickard Brånemark , MD, PhD; P-I Brånemark, MD, PhD; Björn Rydevik, MD, PhD; Robert R. Myers, PhD; “Osseointegration in skeletal reconstruction and rehabilitation” *Journal of Rehabilitation Research and Development, Volume 38, Issue 2, Pages 175–181, 2001.*
- [5] Amaro Sérgio da SilvaMello^aPamela Letíciados Santos^bAllanMarquesi^cThallita PereiraQueiroz^dRogérioMargonar^dAna Paulade Souza Faloni^d ;
“Some aspects of bone remodeling around dental implants”
- [6] Maiko Haga, Noritaka Fuji, Kayoko Nozawa-Inoue, Shuichi Nomura, Kimimitsu Oda, Katsumi Uoshima, Takeyasumaeda; “Detailed Process of Bone Remodeling After Achievement of Osseointegration in a Rat Implantation Model” *THE ANATOMICAL RECORD Volume 292, Pages 38–47, 2009.*
- [7] Chris Steffi, Zhilong Shi, Chee Hoe Kong, and Wilson Wang;
“Modulation of Osteoclast Interactions with Orthopaedic Biomaterials”, *J. Funct. Biomater., Volume 9, Issue 18, 2018.*
- [8] C. MLNKIN, V.C. MARINHO;
“Role of osteoclast at the Bone-Implant interface”, *Adv Dent Res, Volume 13, Pages 49-56, 1999.*
- [9] JS Kenkre¹ and JHD Bassett²;
“The bone remodelling cycle” *Annals of Clinical Biochemistry, ACB-17-252, 2017.*
- [10] Baohong Zhao¹ and Lionel B Ivashkiv^{1,2};
“Negative regulation of osteoclastogenesis and bone resorption by cytokines and

- transcriptional repressors” Zhao and Ivashkiv Arthritis Research & Therapy, Pages 13-234, 2011.*
- [11] Silvia Spriano , Seiji Yamaguchi , Francesco Baino , Sara Ferraris;
“A critical review of multifunctional titanium surfaces: New frontiers for improving osseointegration and host response, avoiding bacteria contamination”
Acta Biomat., Volume 79, Pages 1-22, 2018.
- [12] Liza J. Raggatt and Nicola C. Partridge;
“Cellular and Molecular Mechanisms of Bone Remodeling”,
THE JOURNAL OF BIOLOGICAL CHEMISTRY, Volume 285, Issue 33, Pages 25103–25108, 2010.
- [13] Tanaka Y, Nakayamada S, Okada Y;
“Osteoblasts and osteoclasts in bone remodeling and inflammation.” Curr Drug Targets Inflamm Allergy, Volume 4, Issue 3, Pages 325-8, 2005.
- [14] MacMillan AK, Lamberti FV, Moulton JN, Geilich BM, Webster TJ - Int J Nanomedicine;
“Similar healthy osteoclast and osteoblast activity on nanocrystalline hydroxyapatite and nanoparticles of tri-calcium phosphate compared to natural bone.”
International Journal of Nanomedicine, Volume 9, Pages 5627–5637, 2014.
- [15] Ghada Al Duboni, Muhamed T. Osman, Balsam I. Taha and Lauy A Muhamed;
“The Potential Role of Inflammatory Cytokines as Useful Diagnostic Indicators in Osseointegrated Dental Implants” World Applied Sciences Journal, Volume 20, Issue 5, Pages 649-655, 2012.
- [16] Dulshara Sachini Amarasekara, Hyeongseok Yun, Sumi Kim, Nari Lee, Hyunjong Kim, and Jaerang Rho;
“Regulation of Osteoclast Differentiation by Cytokines Networks” Immune Netw., Volume 18, Issue 1, e8. 2018.
- [17] R.A. Gittens, R. Olivares-Navarrete, R. Tannenbaum, B.D. Boyan, and Z. Schwartz;
“Electrical Implications of Corrosion for Osseointegration of Titanium Implants”
J Dent Res, Volume 90, Issue 12, Pages 1389–1397, 2011.
- [18] Dr. Naveen Reddy Vootla, Dr. K. Varun Reddy;
“Osseointegration- Key Factors Affecting Its Success-An Overview”, IOSR Journal of Dental and Medical Sciences (IOSR-JDMS), Volume 16, Issue 4, Pages 62-68, 2017.

- [19] Rolando A. Gittens, Rene Olivares-Navarrete, Zvi Schwartz, Barbara D. Boyan;
"Implant osseointegration and the role of microroughness and nanostructures: Lessons for spine implants", *Acta Biomater.*, Volume 10, Issue 8, Pages 3363-3371, 2014.
- [20] S. Ferraris, A.Venturello, M.Miola, A.Cochis, L.Rimondini, S.Spriano;
"Antibacterial and bioactive nanostructured titanium surfaces for bone integration"
Acta Biomater., Volume 311, Pages 279-291, 2014.
- [21] Lazzarini L, de Lalla F
"Treatment and prevention of prosthetic joint infections" *Trends Med*, Volume 3, Issue 2, Pages 75-82, 2003
- [22] Suganthan Veerachamy, Tejasri Yarlagaadda, Geetha Manivasagam
"Bacterial adherence and biofilm formation on medical implants: A review"
J Engineering in Medicine, Volume 228, Issue 10, Pages 1083–1099, 2014
- [23] Manuel Simoes a, Lucia C. Simoes b, Maria J. Vieira b
"A review of current and emergent biofilm control strategies" - *Food Science and Technology*, Volume 43, Pages 573–583, 2010
- [24] Muhsin Jamal, Ufaq Tasneem¹, Tahir Hussain¹ and Saadia Andleeb
"Bacterial Biofilm: Its Composition, Formation and Role in Human Infections" *RRJMB*, Volume 4, Issue 3, 2015
- [25] Hans-Curt Flemming and Jost Wingender
"The Biofilm Matrix" *Nature Reviews Microbiology*, Volume 8, Issue 9, Pages 623-33, 2010. *Tutto +1 a parte [1,2,3]*
- [26] Anna Kędziora, Mateusz Speruda, Eva Krzyżewska, Jacek Rybka, Anna Łukowiak and Gabriela Bugla-Płoskonska
"Similarities and Differences between Silver Ions and Silver in Nanoforms as Antibacterial Agents" *Int. J. Mol. Sci.*, 19, 444, 2018.
- [27]
- [28] Sonja Eckhardt, Priscilla S. Brunetto, Jacinthe Gagnon, Magdalena Priebe, Bernd Giese, and Katharina M. Fromm,
"Nanobio Silver: Its Interactions with Peptides and Bacteria, and Its Uses in Medicine" *Chem. Rev.* 2013, 113, 4708–4754.
- [29] Linda Pauksch, Marcus Rohnke, Reinhard Schnettler, Katrin S. Lips
"Silver nanoparticles do not alter human osteoclastogenesis but induce cellular uptake" *Toxicology Reports* 1 (2014) 900–908

- [30] Coathup M; Shawcross J; Scarsbrook C; Korda M; Hanoun A; Pickford M; Agg P; Blunn GW.
“Osseointegration of Silver Treated Titanium Alloy” Poster No. 1549, ORS 2011 Annual Meeting
- [31] Wen-Ta Li 1 , Lei-Ya Wang 1 , Hui-Wen Chang 1 , Wei-Cheng Yang 2 , Chieh Lo 3 , Victor Fei Pang 1 , MengHsien Chen 4 , Chian-Ren Jeng
 Corresp. *“Th2 cytokine bias induced by silver nanoparticles in peripheral blood mononuclear cells of common bottlenose dolphins (Tursiops truncatus)”*
- [32] C. Parnsamut and S. Brimson
“Effects of silver nanoparticles and gold nanoparticles on IL-2, IL-6, and TNF- α production via MAPK pathway in leukemic cell lines”
Genet. Mol. Res. 14 (2): 3650-3668 (2015)
- [33] Alaa Fehaid and Akiyoshi Taniguchi
“Silver nanoparticles reduce the apoptosis induced by tumor necrosis factor- α ”
- [34] Ruizhong Zhang, Puiyan Lee, Vincent C.H.Lui, et al.
“Silver nanoparticles promote osteogenesis of mesenchymal stem cells and improve bone fracture healing in osteogenesis mechanism mouse model”
Nanomedicine: Nanotechnology, Biology and Medicine
Volume 11, Issue 8, November 2015, Pages 1949-1959
- [35] Seung-Heon Shin, Mi-Kyung Ye, Hae-Sic Kim Hyung-Suk Kang
“The effects of nano-silver on the proliferation and cytokine expression by peripheral blood mononuclear cells”
International Immunopharmacology 7(13):1813-8
- [36] Hongjun Xie, Pei Wang & Jie Wu
“Effect of exposure of osteoblast-like cells to low-dose silver nanoparticles: uptake, retention and osteogenic activity” *ARTIFICIAL CELLS, NANOMEDICINE, AND BIOTECHNOLOGY 2019, VOL. 47, NO. 1, 266-267*
- [37] Jingyu Liu, Zhongying Wang, Frances D. Liu, Agnes B. Kane, and Robert H. Hurt
“Chemical Transformations of Nanosilver in Biological Environments”
ACS Nano. 2012 Nov 27; 6(11): 9887–9899.
- [38] Katarzyna Markowska, Anna M. Grudniak and Krystyna I. Wolska
“Silver nanoparticles as an alternative strategy against bacterial biofilms”
Acta ABP Vol. 60, No 4/2013 523–530
- [39] Woo Kyung Jung, Hye Cheong Koo, Ki Woo Kim, Sook Shin, So Hyun Kim and Yong Ho Park *“Antibacterial Activity and Mechanism of Action of the Silver Ion in Staphylococcus aureus and Escherichia coli” APPLIED AND*

- [40] Danielle McShan, Paresh C. Ray, Hongtao Yu
“Molecular toxicity mechanism of nanosilver”
Journal of food and drug analysis 22 (2014) 116-127
- [41] Christina Greulich, Dieter Braun, et al.
“The toxic effect of silver ions and silver nanoparticles towards bacteria and human cells occurs in the same concentration range”
RSC Advances, 2012, 2, 6981–6987
- [42] Victor T. Noronha, Amauri J. Paula et al.
“Silver nanoparticles in dentistry”
Dental Material 33 (2017) 1110 – 1126
- [43] Tianlu Zhang, Liming Wang, [...], and Chunying Chen
“Cytotoxic Potential of Silver Nanoparticles”
Yonsei MED J. 2014 Mar 1; 55(2): 283-291
- [44] Young-Man Cho, Yasuko Mizuta et al.
“Size-dependent acute toxicity of silver nanoparticles in mice”
J Toxicol Pathol 2018; 31: 73–80
- [45] Matthew Charles Stensberg, Qingshan Wei et al.
“Toxicological studies on silver nanoparticles: challenges and opportunities in assessment, monitoring and imaging”
Nanomedicine (Lond). 2011 July ; 6(5): 879–898. doi:10.2217/nnm.11.78.
- [46] D.J. Blackwood, R. Greef, L.M. Peter,
Electrochim. Acta, 34 (1989) 875-880.
- [47] F. El-Taib Heakal, A.A. Ghoneim, A.S. Mogoda, Kh.M. Awad,
Corros. Sci., 53 (2011) 2728-2737.
- [48] F. El-Taib Heakal, Kh.A. Awad
“Electrochemical Corrosion and Passivation Behavior of Titanium and Its Ti-6Al-4V Alloy in Low and Highly Concentrated HBr Solutions”
Int. J. Electrochem. Sci., 6 (2011) 6483 – 6502
- [49] Fey Yu
“CORROSION OF TITANIUM FOR BIOMEDICAL APPLICATIONS”
- [50] Dorian A. H. Hanaor, Charles C. Sorrell
“Review of the anatase to rutile phase transformation”
J Mater Sci (2011) 46:855–874
- [51] Majid H.A., Slafa I.I.
“Corrosion Behaviour of Ti6Al4V alloy in different Media”
Al-K Engineering Journal, Vol.6, No.3, PP 77-84(2010)

- [52] Zhang Yue, Addison Owen, Yu Fei, Rincon Troconis Brendy, R. Scully, John, Davenport, Alison.
“Time-dependent Enhanced Corrosion of Ti6Al4V in the Presence of H₂O₂ and Albumin” Scientific Reports, 2018.
- [53] Maurer-Ertl W. et al
“Recall of the ASR XL head and hip resurfacing systems” Orthopedics 40, e340-e347 (2017)
- [54] Yolanda S. Hedberg
“Role of proteins in the degradation of relatively inert alloys in the human body” Npj Materials Degradation (2018)2:26
- [55] Guisen Wang, Yi Wan*, Teng Wang, Zhanqiang Liu
“Corrosion Behavior of Titanium Implant with different Surface Morphologies” Procedia Manufacturing 10 (2017) 363 – 370
- [56] MasoudRokniana et al
“Study of the effect of ZnO nanoparticles addition to PEO coatings on pure titanium substrate: Microstructural analysis, antibacterial effect and corrosion behavior of coatings in Ringer's physiological solution” Journal of Alloys and Compounds Volume 740, 5 April 2018, Pages 330-345
- [57] Py Palmqvist, Pernilla Lundberg
“Inhibition of Hormone and Cytokine-stimulated Osteoclastogenesis and Bone Resorption by Interleukin-4 and Interleukin-13 Is Associated with Increased Osteoprotegerin and Decreased RANKL and RANK in a STAT6-dependent Pathway” The Journal of Biological Chemistry 281, 2414-2429, 2006

Chapter 5

5. Materials and Methods

5.1. Samples Preparation

For this work Ti6Al4V alloy ASTM B348-10 Grade 5 was used. The specific chemical composition is reported below.

Table 5.1 Chemical Composition of the titanium alloy

Requirement (Max)	Fe max	C max	N max	H max	O max	Al	V	Y max	each	total	Ti
	0,40	0,08	0,05	0,015	0,20	5,5 - 6,75	3,5 - 4,5	-	0,10	0,40	Balance
Result	0,13	0,011	0,01	0,002	0,15	6,11	4,12	-	<0,10	<0,40	Balance

Table 5.2 Tensile strength of the titanium alloy

Requirement min	Tensile Strength [Mpa]	Yield Strength, 0,2% [Mpa]	Elongation 4D [%]	Reduction of Area [%]
	895	828	10	25
Result	985	968	21.5	53

Ti6Al4V is an $\alpha+\beta$ alloy, in which Al is the stabilizer of α phase and gives the alloy excellent properties at high temperature. Instead, the primary function of vanadium is to stabilize the beta phase making improvement of mechanical characteristics with heat treatment possible. As we can notice from *Figure 5.1* pure titanium has a lower Young Modulus (E) and a lower tensile strength (σ_{\max}) but a higher formability than its alloy [1]. That's why Ti6Al4V is today more commercially used as compared to titanium in orthopaedic and dental applications. Particularly, in *Table 5.2* the mechanical characteristics of the alloy used in this thesis is shown.

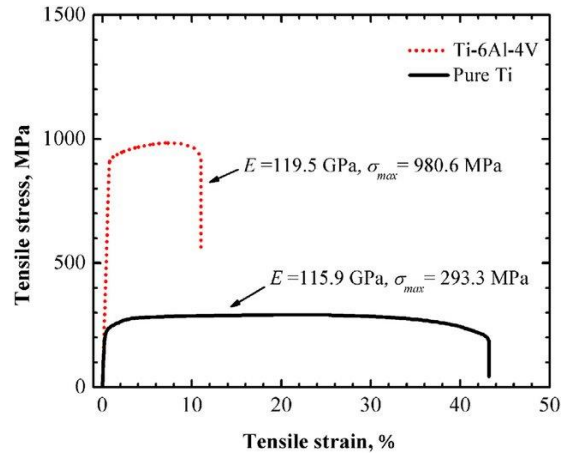


Figure 5.1 . Tensile stress-strain curves of Ti6Al4V alloy and pure titanium, depicted from [1]

The specimens are in the form of disk of 2 mm of thickness and 10 mm of diameter (*Figure 5.3*)

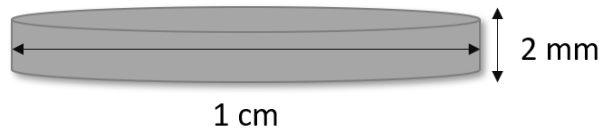


Figure 5.3 . Illustration of Ti6Al4V specimen geometry used in this study

The samples already cut were marked with an electric pen on the back side and subsequently polished on the unmarked side with a polishing machine model Struers “LaboPol-2”, using sequential grades of SiC abrasive papers with water as a lubricant. In particular, 30 samples were ground with grits from P120 through P320 to P400 prior to subsequent treatment. Furthermore, 5 samples were mirror polished from P120, through P320, P400, P600, P800, P1200 to P2500 grit and with diamond abrasive paste.

In *Table 5.3*, the polishing steps for the different samples are reported.

Table 5.3 Polishing steps for different samples

Samples Name	Number of Samples	Polishing
Ti6Al4V_MP	5	Up to 2500 grit on only one side + Diamond abrasive paste 3 μm and 1 μm
Ti6Al4V_Treated	10	Up to 400 grit on only one side
Ti6Al4V_Treated_Ag	20	Up to 400 grit on only one side

After polishing, samples were washed one time in acetone, and two times in Milli-Q (ultrapure) water subsequently using ultrasonic agitation for 5 and 10 min in an ultrasonic bath (Sonica 2400 ETH S3), respectively, with the aim of removing the deposits of silicon created during the previous step.

5.2. Surface Treatments

Surface treatments were carried out in order to improve the bone integration (osseointegration), the biocompatibility, enriching the surface with hydroxide groups and increasing the microroughness, and to provide the titanium alloy with bioactive and antibacterial properties. 5 samples have not been treated but have been investigated for comparative reasons

The process consisted of:

1. *Acid etching* to remove the native oxide (TiO_2 , with a thickness around 10 nm)
2. *Controlled oxidation* which has the aim to form a new layer of thicker and rougher oxide with a different crystalline structure than before ($\text{H}_2\text{Ti}_3\text{O}_7$, with a thickness around 300 nm)
3. *Silver addition* which has the aim to improve the antibacterial properties.

Table 5.4 Treatment for different samples

Samples Name	Number of Samples	Treatment
Ti6Al4V_MP	5	<i>No Treatment, mirror polished</i>
Ti6Al4V_Treated	10	<i>Acid etching, controlled oxidation</i>
Ti6Al4V_Treated_Ag	20	<i>Acid etching, controlled oxidation with addition of silver</i>

The *acid etching process* consisted of the immersion of the samples in 5 mL diluted hydrofluoric acid (HF, 5M) at room temperature for 1 min.

The *controlled oxidation process* consisted of the immersion of the samples in 10 mL hydrogen peroxide (H_2O_2 , 4.2 vol%) at 60 °C in a thermostatic bath (Julabo,

SW23) with a shaking at 120 rpm for 1.5 h.

The *silver addition process* consisted of adding a silver nitrate solution (0.001 M AgNO₃, Silver Nitrate PA-ACS-ISO 131459,1611, Panreac) in hydrogen peroxide in the middle of the previous process (after 45 min).

Simultaneously 2 additives (GA, 0.1 g/L, with a final concentration of 0.1 g/L), a stabilizing agent, and polyvinyl alcohol (PVA, 0.1 g/l, with a final concentration of 0.01 g/L), a reducing agent, were added together with the silver nitrate solution.

The role of the two additives is to control the size of the nanoparticles and to confer the steric stability of the nanoparticles, respectively, in order to control their distribution and ion release.

The concentration of silver (0.001 M) was chosen, because that concentration was non-cytotoxic based on literature.

The solvent for all processes above was ultrapure water.

After the treatment, even for the one without treatments, all samples were placed in the laminar flux hood for drying and were finally packed in closed plastic bags and brought to the laboratories at KTH (Royal Institute of Technology in Stockholm).

The preparation and treatments of all the samples were carried out in the laboratories at the Politecnico di Torino.

5.3. Surface Characterization

5.3.1. SEM

The surface topography was analysed by means of scanning electron microscopy (SEM, PHILIPS XL30ESEM) (*Figure 5.4*).



Figure 5.4 . SEM used during this study

Two different kinds of electrons are created in this SEM:

- Secondary electrons (SE)
- Back scattered electrons (BSE)

The typical energy of the secondary electrons is < 50 eV and they are ejected from a depth of a few nm. They result from inelastic interactions between the primary electron beam and the sample. For these reasons, the secondary electrons are very useful for the topographic analysis of the sample. The energy of the backscattered electrons is higher than secondary electrons and they are generated from a deeper zone of the sample. They result from elastic collisions between electrons and atoms,

collisions that induce electron trajectory changes. Therefore, the backscattered electrons are used to have information about the composition of the sample. To get information about the chemical composition of the sample, the instrument is equipped with Energy Dispersive X-ray Spectroscopy (EDS, XMAX Oxford instruments, 20 mm² detect). The technique is based on the detection of characteristic X-rays that emitted from the electrons during collisions with different atoms. In the figure below (*Figure 5.5*) the different interactions just explained are represented.

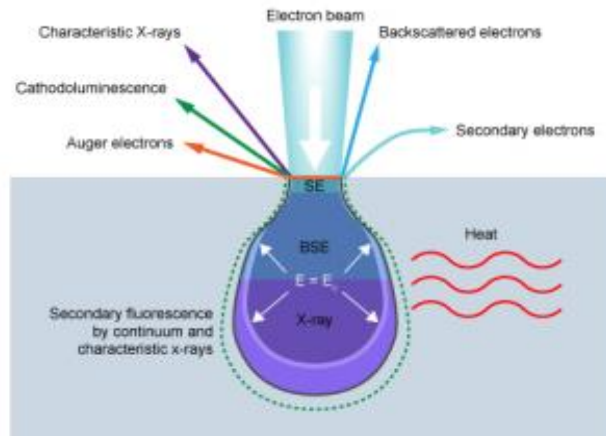


Figure 5.5 . Different interactions between the beam and the sample [2]

Mirror polished samples (Ti6Al4V_MP), treated samples (Ti6Al4V_Treated) and samples treated with silver (Ti6Al4V_Treated_Ag) were analysed in the SEM before and after the different tests, with the three methods of analysis explained, to have all the necessary information completely. The SEM was even used for the analysis of the cross-sections. For this, a cross section was made. First, the sample was embedded in epoxy resin. Then, it was ground perpendicular to its surface until a desired depth was obtained. Finally, it was cleaned in an ultrasonic bath in acetone and ethanol, subsequently.

5.3.2. Profilometry

Since the roughness is an important parameter which can affect the success of the implant and give insights on the treatment processes, it was measured through a Stylus Profiler (Bruker Dektak XT Precision) (*Figure 5.6*) to see if there is any difference of roughness between each sample.

For each sample, three different points were chosen and the diamond stylus measured three lines of 1 mm length from the points.



Figure 5.6 . Bruker Dektak XT Precision Profilometer

Once the measurement is done, and all the parameters are calculated through the software Vision 64, an average between 3 different points and its standard deviation was made. Among all the parameters calculated, the arithmetical mean height (R_a) has been taken into consideration. The arithmetical mean height indicates the average of the absolute value along the length of the measured line (*Figure 5.7*):

$$R_a = 1/lr \int_0^{lr} |Z(x)| dx$$

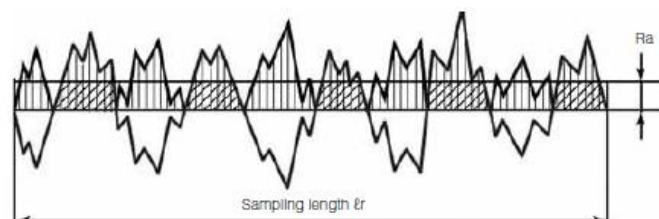


Figure 5.7 . Arithmetical mean height

In the table below (*Table 5.4*) there is the procedure showing which and how many samples were measured by profilometry.

Table 5.4 Samples measured by profilometry

ID Sample	Test before Profilometry	Number of samples	Parameters calculated during profilometry	Subsequent calculations after profilometry
Ti6Al4V_MP	Not exposed	2	Ra	Average + st. dev
Ti6Al4V_Treated	Not exposed	2	Ra	Average + st. dev
Ti6Al4V_Treated_Ag	Not exposed	3	Ra	Average + st. dev
Ti6Al4V_Treated	PBS	2	Ra	Average + st. dev
Ti6Al4V_Treated_Ag	PBS	3	Ra	Average + st. dev
Ti6Al4V_Treated	PBS+BSA	2	Ra	Average + st. dev
Ti6Al4V_Treated_Ag	PBS+BSA	3	Ra	Average + st. dev
Ti6Al4V_Treated	PBS+BSA+H2O2	2	Ra	Average + st. dev
Ti6Al4V_Treated_Ag	PBS+BSA+H2O2	3	Ra	Average + st. dev
Ti6Al4V_MP	PBS+H2O2+BSA	1	Ra	Average + st. dev
Ti6Al4V_Treated	PBS+H2O2+BSA	2	Ra	Average + st. dev
Ti6Al4V_Treated_Ag	PBS+H2O2+BSA	3	Ra	Average + st. dev

5.3.3. Colorimetry

A colorimetric measurement was carried out inspired by a visible variety of the colors of the sample surfaces. Generally, metal surfaces often appear colored and sometimes this occurs because they could be covered by patinas of corrosion products, after exposure to aggressive conditions. In the case of titanium, the color is due to the presence of thin transparent layers of the surface oxide capable of producing an interference phenomenon of light. Normally, titanium is covered with a protective oxide film of a few nanometers in thickness. Through the acid and oxidation treatment, the thickness of the oxide film increased together with the roughness, parameters which affect visibly the surface color of the samples. The colors produced are hence caused by interferences that depend on the surface texture (including the thickness) and not on the presence of pigments.

The instrument used for colorimetry interprets the colors in CIELAB coding giving as output 3 coordinates ($L^*a^*b^*$) which indicate the position of the color in the color space lab. As can be seen from the *Figure 5.8*, L represents the lightness, and a and b are termed opponent color axes: a represents redness (positive) versus greenness (negative) and b represents the yellowness (positive) versus blueness (negative).

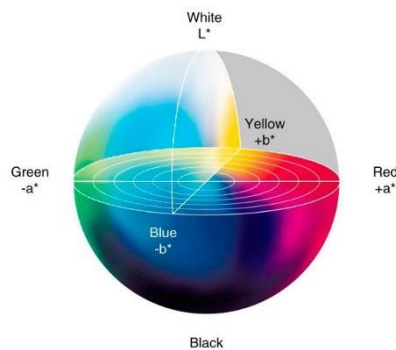


Figure 5.8 . CIELAB space

5.4. Experimental Plan

5.4.1. Electrochemical Test

5.4.1.1. Setting

All the prepared samples, in order to evaluate the corrosion of the alloy, were subjected to an electrochemical test, through PARSTAT MC Multichannel Potentiostat (*Figure 5.9*), with the aim to measure:

- OCP: Open Circuit Potential, could be explained as the voltage measured when no current flows through the cell. The OCP reflects the thermodynamic parameter that indicates how much that specific metallic material tends to participate in electrochemical corrosion with the adjacent medium (which in our case is the electrolyte). Therefore, a potential under OCP is more thermodynamically stable (less corrosion tendency) while the potential above the OCP is thermodynamically unstable and subjected to corrosion. It is good practice to monitor the OCP of a test before starting a potentiodynamic test or other tests in order to be able to verify that the sample has reached at least a balance with the test solution. Otherwise, no reproducible results can be obtained. Also, changes of OCP versus time can to some extent give information on electrochemical reaction kinetics at no applied potential.

The setting parameters used for OCP were:

- Duration: 604 800 s
- Time per point: 5 s
- Current range: Auto
- Temperature: 37 ± 1 °C

- EIS (Electrochemical Impedance Spectroscopy): These measurements were taken after one week of OCP. This test measures the resistance and the capacitance of a material immersed in an electrolyte, applying and varying the frequency in a defined range.
 - Frequency range: 0.1 to 10000 Hz
 - RMS: 10 mV
 - Acquisition rate: 10 points per decade
 - Temperature: 37 ± 1 °C

In our case, the Nyquist plot (Z_{re} , $-Z_{im}$) is mainly taken into consideration because it provides the following information:

- At low frequencies, it's possible to understand, from the angle with the X axis, if the material is purely capacitive (in this case the Nyquist plot is a vertical line, or it presents diffusive effects (with a maximum of 45° if it's purely diffusive)
 - At high frequencies, the Nyquist plot looks like a semicircle and, starting from a model, it is possible to calculate the resistances and capacities involved.
- PD (Potentiodynamic polarization): This test was conducted in the end of a test series, since it is a destructive test.

In this technique, the voltage is applied and varied with a selected rate and the current which flows through the cell is measured.

In our case, the potentiodynamic curve is composed of three zones:

- Cathodic zone (which is at more negative potentials compared to the corrosion potential and it's dominated by the cathodic reaction, therefore the reaction depends mainly on the electrolyte)
- Anodic zone (which is more positive to the corrosion potential and it's dominated by the anodic reaction, which means that on the surface of the metal, an active reaction starts and the working electrode becomes an anode)
- Passive zone (in this zone, a passive layer on the surface of the sample is created, or already present, which means that there is very limited current flow, and as the potential increases, the current remains constant).

The importance of the potentiodynamic polarization is represented by the ability to identify and understand the reaction, and the processes which create and stabilize the passive film. Through the potentiodynamic polarization curves, E_{corr} (the corrosion potential, which is the OCP of balance during the potentiodynamic test) and i_{corr} (the corrosion current density in A/cm^2) were evaluated by using the Tafel extrapolation method.

The setting parameters used for the potentiodynamic polarization were:

- Initial potential: -0.2V vs OCP
- Final potential: 1 V vs OCP
- Step height: 3 mV, step time: 5 s
- Scan rate: 0.6 mV
- Current range: 2 μA
- Temperature: 37 ± 1 °C



Figure 5.9: PARSTAT MC Multichannel Potentiostat

5.4.1.2. Simulated physiological fluid

Physiological solutions were based on phosphate buffered saline (PBS) with varying hydrogen peroxide (H₂O₂, Sigma Aldrich, Sweden) and bovine serum albumin (BSA, A7906, Sigma Aldrich) concentrations. The exposures were carried out during one-week time periods (168 h), the components of the different testing solutions were added gradually (every 24 h until the solution was complete). Four different solutions were considered depending on their contents and the order of the added components:

Table 5.4 Tested artificial body fluids. The concentrations show final concentrations.

Solution name	Adding order	Final Volume
A	PBS	45mL
B	PBS + BSA (40g/L)	45mL
C	PBS + BSA (40g/L) + H ₂ O ₂ (30mM)	45mL
D	PBS + H ₂ O ₂ (30mM) + BSA (40g/L)	45mL

Phosphate buffered saline (PBS) was composed of 8.77 g/L NaCl, 1.28 g/L Na₂HPO₄, 1.36 g/L KH₂PO₄ in ultrapure water, and its pH was adjusted to 7.2-7.4 with 50%

NaOH. Albumin is the most abundant protein in the human body and 40 g/L is a relevant concentration for human blood, whereas an amount of 30mM of H₂O₂ is representative of inflammatory conditions: some particular conditions involving macrophages and other neutrophils have very oxidative properties, and it has been shown that a 30 mM concentration of H₂O₂ has a strong effect and is relevant for worst-case scenarios in-vivo [3].

5.4.1.3. Set-up trouble shouting

One of the main challenges in this project was the electrochemical setup.

The **first set-up** chosen included:

- Reference electrode: Ag/AgCl saturated with KCl
- Counter electrode: Wire of platinum (Pt)
- Working electrode: Prepared samples
- Electrochemical cell, as seen in *Figure 5.11*, which consisted of a 35 mL (0.022 cm²/mL loading) glass vessel in which the electrolyte, the reference electrode, the counter electrode and the working electrode are placed.
- Electrolyte: see Table 5.4.

In order to effectively connect the disk-shaped sample to the electrochemical cell, a platinum wire was fixed on the back side of the disk using adhesive carbon tape.

This side, in addition to the edges of the disk, were then entirely covered with metal-free nail polish so that only one face (0.785 cm^2) was exposed (*Figure 5.10*).



Figure 5.10: First sample preparation

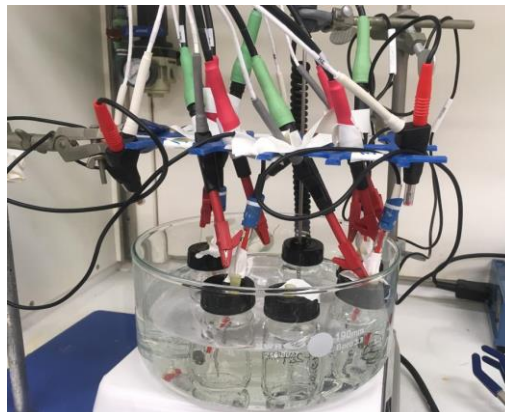


Figure 5.11: First electrochemical set-up

Each sample was tested in a single vessel which was placed in a $37 \text{ }^\circ\text{C}$ water bath, relevant for human body temperature.

However, the obtained values were much higher (approx. 250 mV) than what was expected or what was found in the literature at those conditions (approx. -300 mV) [4,5].

This difference could be due to contributing currents and/or a high contact resistance (magnifying the effect of small leakage currents) in the setup.

In order to solve this issue, several other setups were tested with an already used (previous study) Ti6Al4V_MP sample. The sample was exposed in a similar glass vessel, containing only PBS, and using an identical reference electrode. Then the OCP was measured for a few minutes with different means of contact between the sample and the potentiostat.

At the end, a proper set-up was found, which gave the expected OCP values. It was decided to remove the carbon tape which did not ensure proper contact between

the platinum and the sample, and it was decided to instead apply more force through a copper slab that ensured electrical connection with the potentiostat.

Then, the **new set-up** included:

- Reference electrode: Ag/AgCl saturated with KCl
- Counter electrode: Mesh of Platinum (Pt)
- Working electrode: Prepared Samples
- Electrochemical cell, which consisted a home-made flat cell with the electrolyte, the reference electrode, the counter electrode and the working electrode.
- Electrolyte: Same as before.

5.4.1.4. Home-made flat cell

Before the assembly, all vessels and equipment necessary to build the flat cell were acid-cleaned in 10% HNO₃, for at least 24 h, rinsed 4 times with ultrapure water (18.2 MΩcm, Millipore, Sweden) and then dried in the air of the laboratory. The flat cells consisted in a 50 mL plastic vessels in which a hole was made with an o-ring stuck upon it, to avoid leakage problems. The working electrode (the sample) was leaned against the o-ring and held in place by a copper slab which, in turn, was held with a very tight elastic band. The copper slab ensured connection between the sample and the crocodile clamp, connected to the potentiostat, while the elastic band ensured a contact force between the sample and the copper slab. The reference and counter electrodes were placed in the plastic vessels. *Figure 5.12* below represents an illustration of the flat cell. In this way, only one side of the sample was exposed to the solution, and the exposed area (A_e) was 0.502 cm².

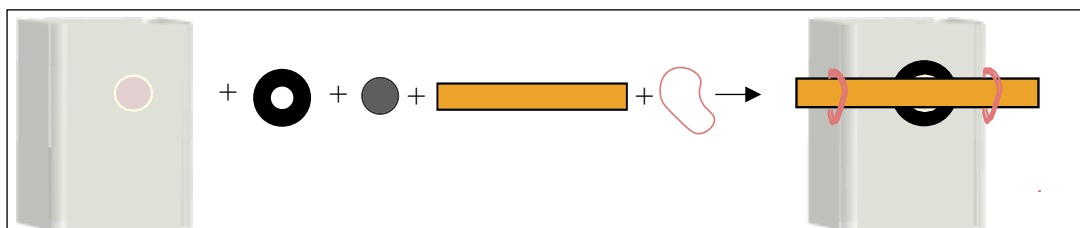


Figure 5.12: Illustration of the flat cell

5.4.1.5. Electrochemical test's plan

The research project focused on the effect of albumin and hydrogen peroxide on the corrosion behaviour of the treated samples. The focus was to investigate the differently treated samples in three-electrode electrochemical cells with the four different solutions as electrolytes, in order to measure the open-circuit potential (OCP) for one week before starting the EIS measurements, ending up with potentiodynamic measurements for each specimen. For each solution, different experimental plans were used. For the solutions A and D (PBS and PBS+H₂O₂+BSA, respectively), EIS and potentiodynamic polarization measurements were made after the OCP. For the solutions B and C (PBS+BSA and PBS+BSA+H₂O₂, respectively), only OCP measurements were conducted (*Table 5.5*).

Table 5.5 Order of measurements depending on the solution

Solution Name	First measurement	Second measurement	Third measurement
PBS	OCP	EIS	PD
PBS+BSA	OCP	-	-
PBS+BSA+H₂O₂	OCP	-	-
PBS+H₂O₂+BSA	OCP	EIS	PD

In general, all the electrochemical cells were immersed in a thermal bath in which the temperature was maintained at 37 ± 1 °C and at the end of all the measurements, all the samples were rinsed with 0.5 mL of ultrapure water, dried with nitrogen gas and stored ready to be analysed with the SEM. The test solutions and their corresponding 0.5 mL of rinsing water were combined and stored at -20°C, before they were digested by UV or micro wave digestion and analyzed by GF-AAS.

5.4.2. Metal Release

5.4.2.1. Microwave digestion

To ensure an accurate analysis of the metal release by GF-AAS, all the solutions were digested in order to avoid silver precipitation and protein aggregation. Unfrozen solutions were diluted by adding 5 mL of 65% nitric acid (HNO_3) and 3 mL ultrapure water to 2 mL of solution sample and then digested using Milestone Ultraclave for about 30 min at 180°C until the solution was transparent and odorless. After the digestion process, and after measuring the final volume, the dilution factor was calculated (final volume after digestion divided by the volume of the initial solution).

5.4.2.2. Atomic absorption spectroscopy

Atomic absorption spectroscopy (AAS) is a technique to measure the quantities of metallic elements present in solutions in which metal samples have been exposed (Figure 5.13).

The presence of the metal is detected measuring the radiation absorbed by the element of interest.

The total concentrations ($\mu\text{g/L}$) of Ti, Al, V and Ag in the solutions were measured by means of graphite furnace atomic absorption spectroscopy (GF-AAS) using a Perkin Elmer AA800 analyst instrument. It was calibrated for each metal using standard concentrations of nitric acid as seen in the table below (Table 5.6)

Table 5.6 AAS calibration standard concentrations for the studied metals

Metal	standard concentrations for calibration
Ti	0, 30, 60 and 80 $\mu\text{g/L}$
Al	0, 30, 60 and 100 $\mu\text{g/L}$
V	0, 10, 30, 80 and 120 $\mu\text{g/L}$
Ag	0, 7.5, 15, 20 and 45 $\mu\text{g/L}$

Every 4 or 5 samples, quality control samples of known concentrations were analysed, and ultra-pure water was analysed every 2 or 3 samples to avoid memory effects. After the measurement of the different concentrations, the released and non-precipitated amount of metal Me_{aq} ($\mu\text{g/cm}^2$) can be calculated for each solution as follows:

$$Me_{aq} \left(\frac{\mu\text{g}}{\text{cm}^2} \right) = \frac{\left(c_{sample} \left(\frac{\mu\text{g}}{\text{L}} \right) - c_{blank} \left(\frac{\mu\text{g}}{\text{L}} \right) \right) * V(\text{L})}{A(\text{cm}^2)} * DF$$

In which: c_{sample} represents the measured sample concentration, c_{blank} is the corresponding blank concentration (amount of metal ions revealed into the solution exposed without samples), V is the exposure volume (45 mL), A is the exposed surface area (0.502 cm²) and DF is the dilution factor.



Figure 5.13: AAS instrument

References:

- [1] Yang Zhang, Guo-Rong Ma, Xian-Cheng Zhang
“Thermal oxidation of Ti-6Al-4V alloy and pure titanium under external bending strain: Experiment and modelling” Corrosion Science, January 2017
- [2] Sven Pletincx
“Study of the encapsulation of healing agents for autonomous self-healing coatings.” 2013
- [3] Hedberg Y., Žnidaršič M., Herting G., Milošev I., Odnevall Wallinder I..
*“Mechanistic insight on the combined effect of albumin and hydrogen peroxide on surface oxide composition and extent of metal release from Ti6Al4V”
J Biomed Mater Res Part B, 2018.*
- [4] Zhang Yue, Addison Owen, Yu Fei, Rincon Troconis Brendy, R. Scully, John, Davenport, Alison.
“Time-dependent Enhanced Corrosion of Ti6Al4V in the Presence of H2O2 and Albumin” Scientific Reports, 2018.
- [5] Fei Yu, Owen Addison, Alison J. Davenport
*“A synergistic effect of albumin and H2O2 accelerates corrosion of Ti6Al4V”
Acta Biomater., Volume 79, Pages 1-22, 2018.*

Chapter 6

6. Results

6.1. Surface characterization

6.1.1. SEM

SEM measurements were performed on the different samples in order to get a better understanding of the treatment and its effect on the titanium surface. The morphology of the samples prior and after exposures was investigated as well as their elemental composition (wt-%) by means of EDS.

Mirror polished samples

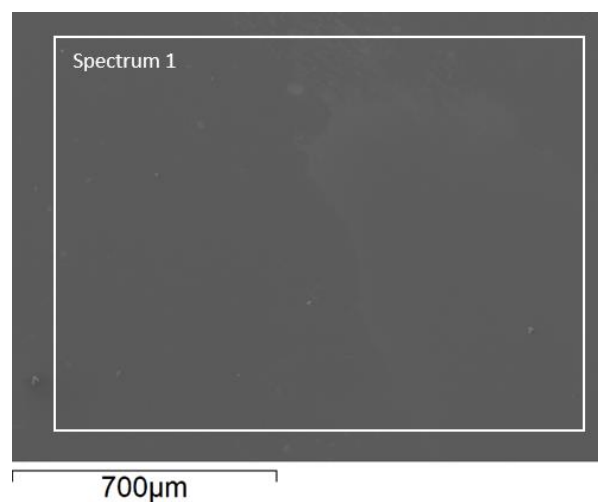


Figure 6.1. SEM BSE images of the surface of Ti6Al4V_MP x1200, before exposure

Table 6.1. EDS analysis of Ti6Al4V_MP (%wt)

Spectrum	C	O	Al	S	Ti	V
Spectrum 1	3.57	-	6.00	-	87.83	2.59

- Fig. 6.1 shows the surface of a Ti6Al4V_MP sample before the exposure. Its texture is remarkably smooth and is considered as a reference for the comparison to the other samples. The EDS results are as expected, with an expected balance between various element and without oxygen.

Treated samples

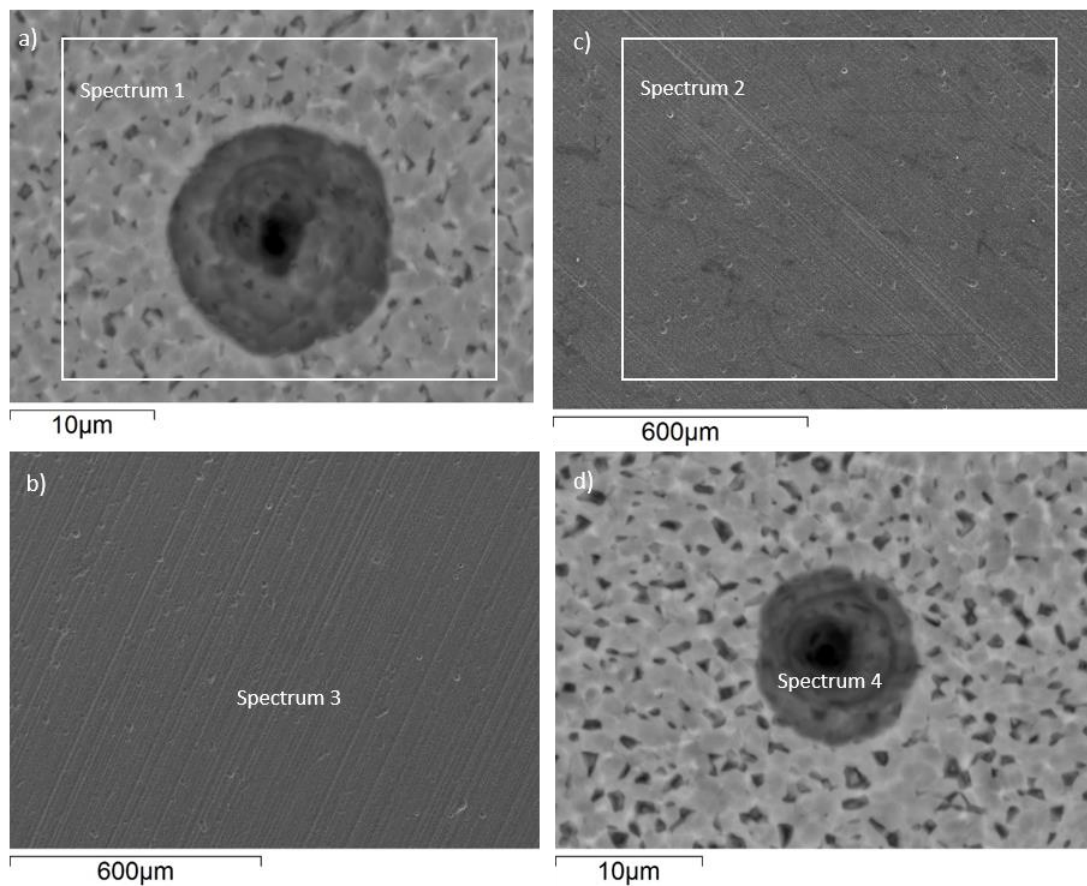


Figure 6.2. SEM BSE images of the surface of Ti6Al4V_Treated (a) x100, before exposure (b) x3500, detail before exposure (c) x100, after exposure (d) x3500, detail after exposure in PBS+BSA+H₂O₂

Table 6.2. EDS analysis of Ti6Al4V_Treated (wt-%)

Spectrum	C	O	Al	Ti	V	K
Spectrum 1	2.98	29.01	3.76	62.18	2.07	-
Spectrum 2	2.49	35.64	3.28	56.62	2.00	-
Spectrum 3	0.64	6.40	0.17	91.13	1.67	-
Spectrum 4	-	10.67	0.33	86.38	2.40	0.22

- Fig. 6.2a shows the surface of a Ti6Al4V_Treated sample before the exposure. Its texture is visibly rougher than that of the mirror polished specimen. The EDS results are as expected, with lower percentage of metallic elements and a higher percentage of oxygen, since the treatment results in a considerable amount of titanium oxide on the top of the surface.
- Fig. 6.2c shows the surface of a Ti6Al4V_Treated sample after the exposure in PBSA+BSA+H2O2 solution. Its texture visibly changed after the electrochemical test.
- Fig. 6.2b/d show details on the surface of a Ti6Al4V_Treated sample before the exposure and after the exposure in PBSA+BSA+H2O2 solution, respectively. These spots are visible on the surface regardless of whether before or after the electrochemical test, since they are particularly created by the treatment. They are characterized by a very low percentage of aluminium, lower percentage of oxygen and an higher percentage of titanium. Evidently, this kind of treatment produces holes scattered on the oxide layer, reaching the bulk zone. Instead, the loss of aluminium can be given by the acid etching process with HF. The presence of potassium (K) on the sample in figure 6.2d, is due to the solution during the exposure, which contains potassium (K) in

PBS. It seems that the other pores become larger after the exposure as compared with prior to exposure (Fig. 6.2d compared with 6.2b).

Treated samples with silver

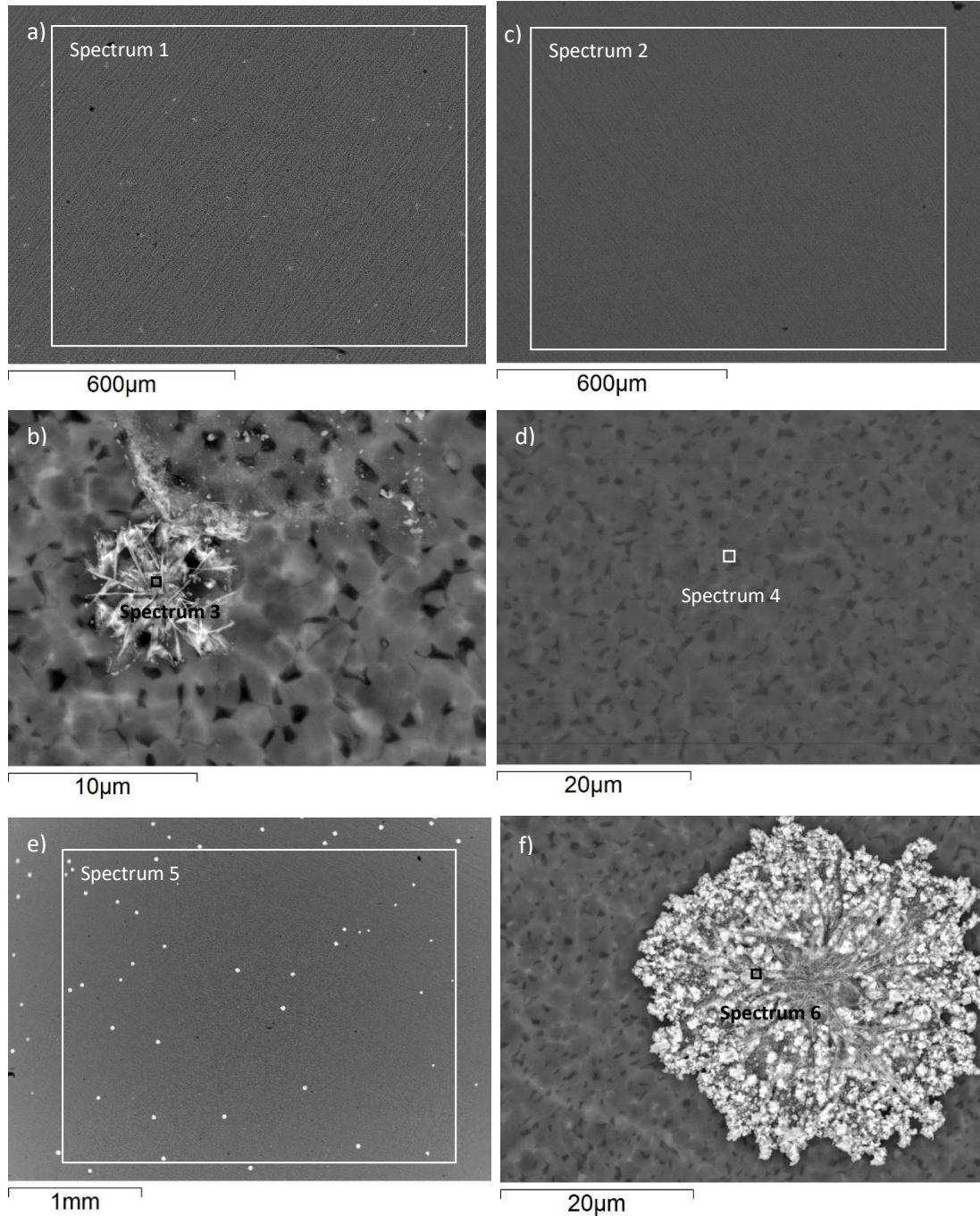


Figure 6.3. SEM BSE images of the surface of Ti6Al4V_Treated_Ag (a) x100, before exposure (b) x3500, detail before exposure (c) x100, after exposure in PBS+BSA+H₂O₂ (d) x2000, detail after exposure in PBS+BSA+H₂O₂, (e) x35, before exposure (f) x2000, detail before exposure
 Table 6.2. EDS analysis of Ti6Al4V_Treated_Ag (%wt)

Table 6.2. EDS analysis of Ti6Al4V_Treated_Silver (wt-%)

Spectrum	C	O	Al	Ti	V	Ag
Spectrum 1	4.97	27.05	4.09	61.55	2.34	-
Spectrum 2	5.29	25.12	3.84	63.35	2.40	-
Spectrum 3	5.46	16.35	3.65	59.41	1.91	13.22
Spectrum 4	4.24	35.64	4.01	54.56	1.56	-
Spectrum 5	4.62	28.73	3.31	60.86	2.47	-
Spectrum 6	-	-	1.19	42.04	1.88	54.88

- Fig. 6.3a shows the surface of a Ti6Al4V_Treated_Ag sample before the exposure. The surface presents visible big particles of silver, of the order of micrometres, which was unexpected, since the treatment should have created an homogeneous distribution of nanoparticle of silver. From EDS results, making an average on the surface, the amount of silver visible on the surface is not detected, which means that in that region particles of silver are not homogeneous and the average calculated is lower than 0.5 % in confront of the other elements.
- Fig. 6.3b shows the detail of the particle of silver presented on the surface; it's possible to see that it is composed of an agglomeration of smaller particles of silver, which suggests that stabilizing agents during functionalization didn't function properly.
- Fig. 6.3c/d show the surface of a Ti6Al4V_Treated_Ag sample and its detail after the exposure in PBSA+BSA+H2O2 solution, respectively. In this case particles of silver are not presented, which means that all (or most) of the silver

was lost during the electrochemical test. For that reason, they didn't seem to be very firmly bound to the surface oxide.

- Fig. 6.3e/f shows the surface of a Ti6Al4V_Treated_Ag sample before the exposure and its detail. This is an emblematic sample that proves the exaggerated particle size, indicating that there were problems during the silver addition process.

6.1.1.1. Cross section

Analysis with the SEM of the cross section of the samples was carried out to study the different treatment layers of samples with and without the Ag treatment and the effect of the least and the most aggressive solutions.

Mirror polished samples

As clear from Figure 6.4a, the mirror polished samples present a very thin oxide layer, which increases in thickness and in compactness after adding H₂O₂ in the solution (Figure 6.4c). It has been shown that H₂O₂ reacts with the titanium surface by forming the oxyhydroxide TiOOH, creating a thicker layer above the surface that increases the roughness and the porosity [1].

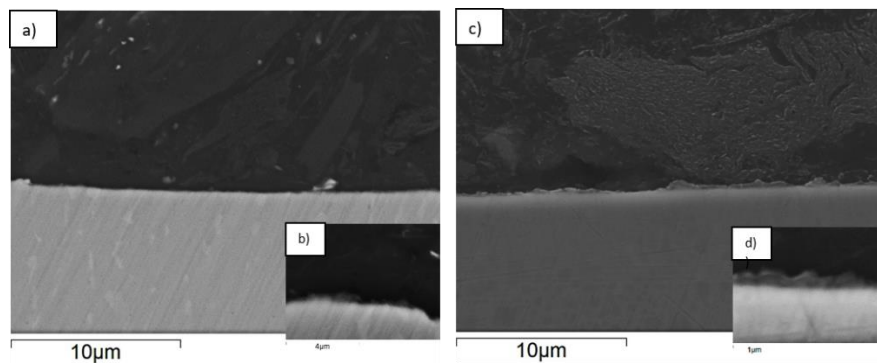


Figure 6.4. SEM BSE, images of the cross section of Ti6Al4V_MP (a) x5000, after exposure in PBS solution (b) x15000, detail (c) x5000, after exposure in PBS+H₂O₂+BSA solution (d) x35000, detail

Treated samples with and without silver

Figure 6.5a shows the treated samples which present a thicker layer of oxide (around ~ 300 nm) as compared with the mirror-polished sample, and the treated samples didn't change visibly upon adding H₂O₂ in the solution (Figure 6.5b). For the treated samples with silver (Figure 6.5b), the layer of oxide is slightly thinner (~200 nm) and visibly less compact, in agreement with the electrochemical results which will be presented in the next paragraph. Every sample presents pits in the substrate probably due to the acid etching process with HF.

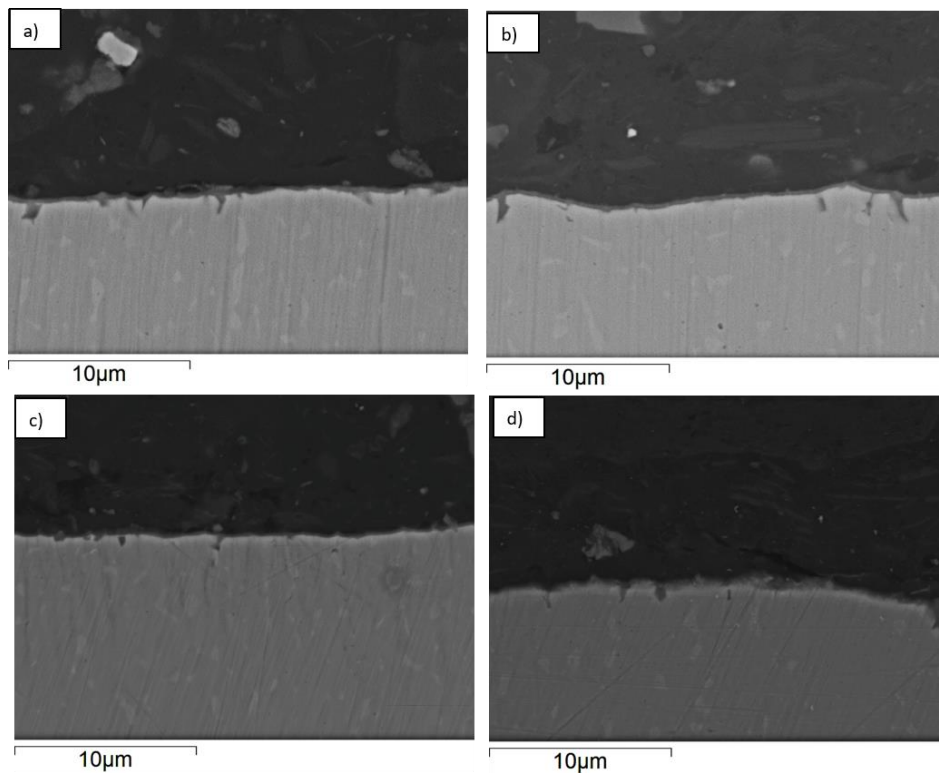


Figure 6.5. SEM BSE, images of the cross section of (a) Ti6Al4V_Treated x5000, after exposure in PBS solution (b) Ti6Al4V_Treated x5000, after exposure in PBS+H₂O₂+BSA solution (c) Ti6Al4V_Treated_Silver x5000, after exposure in PBS solution (d) Ti6Al4V_Treated_Silver x5000, after exposure in PBS+H₂O₂+BSA solution

6.1.2. Profilometry

Profilometry measurements were performed on the different samples (Table 6.3) in order to understand if the electrochemical tests and the various types of solutions used may affect the roughness of the samples.

Table 6.3 Results of profilometry

ID Sample	Test Before	Number of Samples	Ra Average (μm)	Standard Deviation
Ti6Al4V_MP	Not exposed	2	0.05	0.01
Ti6Al4V_Treated	Not exposed	2	0.235	0.012
Ti6Al4V_Treated_Ag	Not exposed	3	0.259	0.0386
Ti6Al4V_Treated	PBS	2	0.231	0.0112
Ti6Al4V_Treated_Ag	PBS	3	0.285	0.0421
Ti6Al4V_Treated	PBS+BSA	2	0.246	0.0133
Ti6Al4V_Treated_Ag	PBS+BSA	3	0.313	0.039
Ti6Al4V_Treated	PBS+BSA+H2O2	2	0.287	0.0113
Ti6Al4V_Treated_Ag	PBS+BSA+H2O2	3	0.294	0.023
Ti6Al4V_MP	PBS+H2O2+BSA	1	0.055	0.008
Ti6Al4V_Treated	PBS+H2O2+BSA	2	0.292	0.0143
Ti6Al4V_Treated_Ag	PBS+H2O2+BSA	3	0.291	0.036

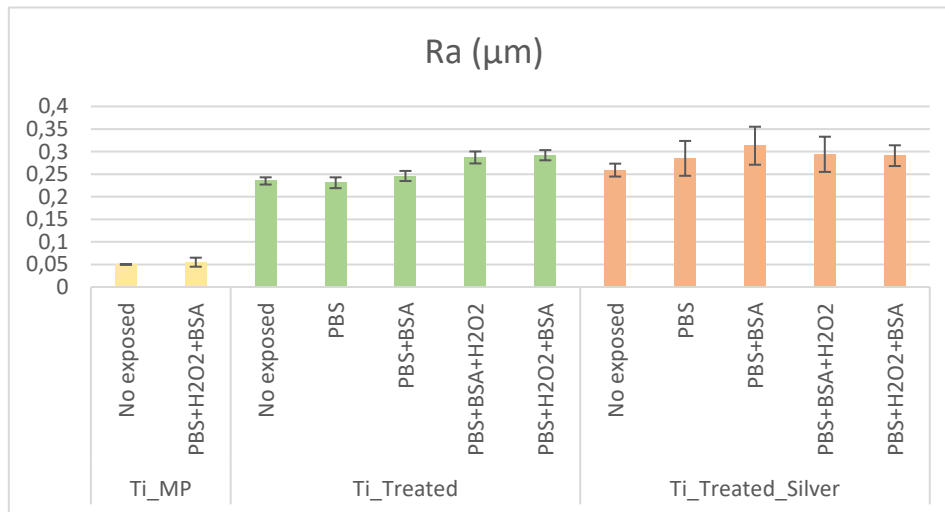


Figure 6.4 Average of arithmetical roughness and its standard deviations.

The results show that the roughness changes slightly depending on the samples and solutions used during the exposure, in particular:

- The mirror-polished samples were characterized by having very low values of arithmetical roughness ($R_a \sim 0.05 \mu\text{m}$), which is as expected as they were polished in order to get a very smooth surface, there is a slight increase in the roughness after the exposure and it could be due to the solution used in this case since the presence of H_2O_2 results in increased porosity and roughness.
- The treated samples without silver are characterized by having higher values of arithmetical roughness ($R_a \sim 0.25 \mu\text{m}$), as compared with the mirror-polished samples, which is expected.

Even in this case, there is a slight increase in the roughness after exposure, in particular after the exposure in which there is the solution with H_2O_2 , which confirms the fact that the peroxide is more aggressive for the surface than the albumin alone, possibly also due to a synergistic effect with the albumin.

- The treated samples with silver have similar values of arithmetical roughness ($R_a \sim 0.30 \mu\text{m}$). In this case, the roughness doesn't strictly follow the same rule as for the samples without silver: even if the roughness has increased slightly upon solution exposure, the standard deviation is visibly higher than without exposure. This could be explained by a more heterogeneous surface due to silver particles and agglomerates.

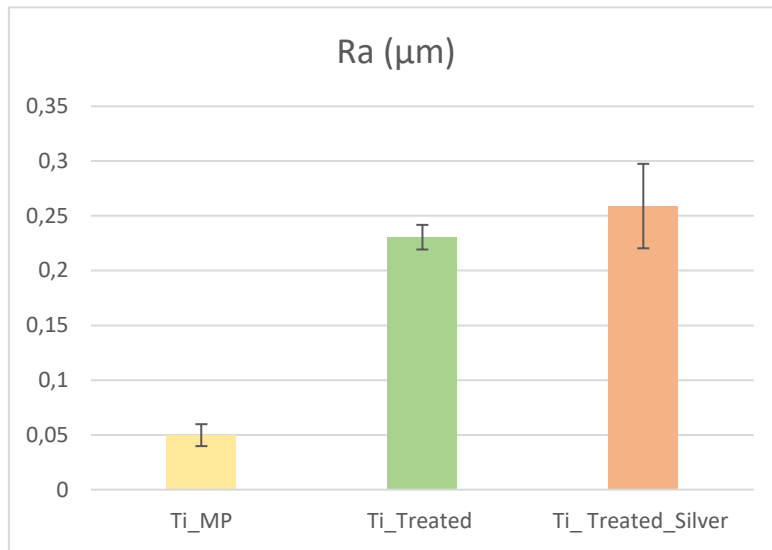


Figure 6.5 Average of arithmetical roughness and its standard deviations for all samples (unexposed and exposed to different solutions).

6.1.3. Colorimetry

To obtain a measure on the variety of the colour of the sample surfaces, colorimetry was carried out before the exposure, providing the output parameters a, b and L.

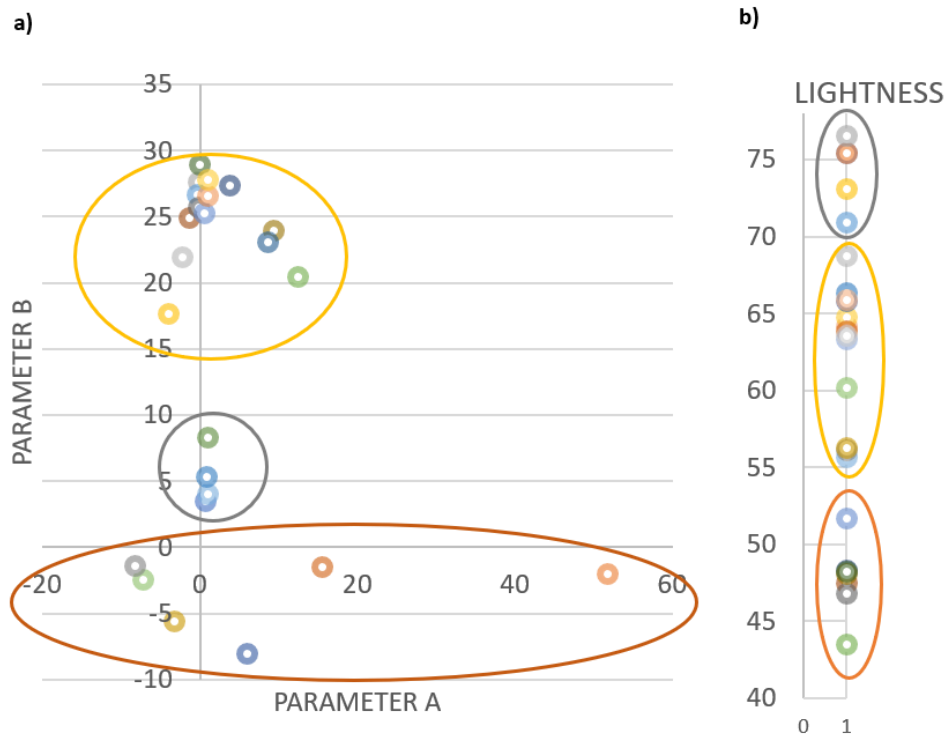


Figure 6.6 CIELAB Space coordinates of Ti6Al4V_MP, Ti6Al4V_Treated, Ti6Al4V_Treated_Ag samples before exposure: (a) (Yellowness, Redness) graph and (b) Lightness Scale

Figure 6.6 shows that there is a correspondence of colour between samples of the same type:

- Ti6Al4V_Treated_Ag (yellow circle) have $15 < b < 30$ and $55 < L < 70$
- Ti6Al4V_MP (grey circle) have $15 < b < 30$ and $55 < L < 70$
- Ti6Al4V_Treated (red circle) have $-10 < b < 0$ and $40 < L < 55$.

The addition of silver, since it happens in the middle of the *controlled oxidation process*, can influence the growth of the layer by interrupting the growth process.

This results in a different color that tends towards yellow (which corresponds to a greater b).

6.1.4. Electrochemical Tests

6.1.4.1. OCP behaviour

OCP measurements were carried out for all samples. Example results are shown for Ti6Al4V_MP and for Ti6Al4V_Treated_Ag with more aggressive solutions in

Figure 6.7.

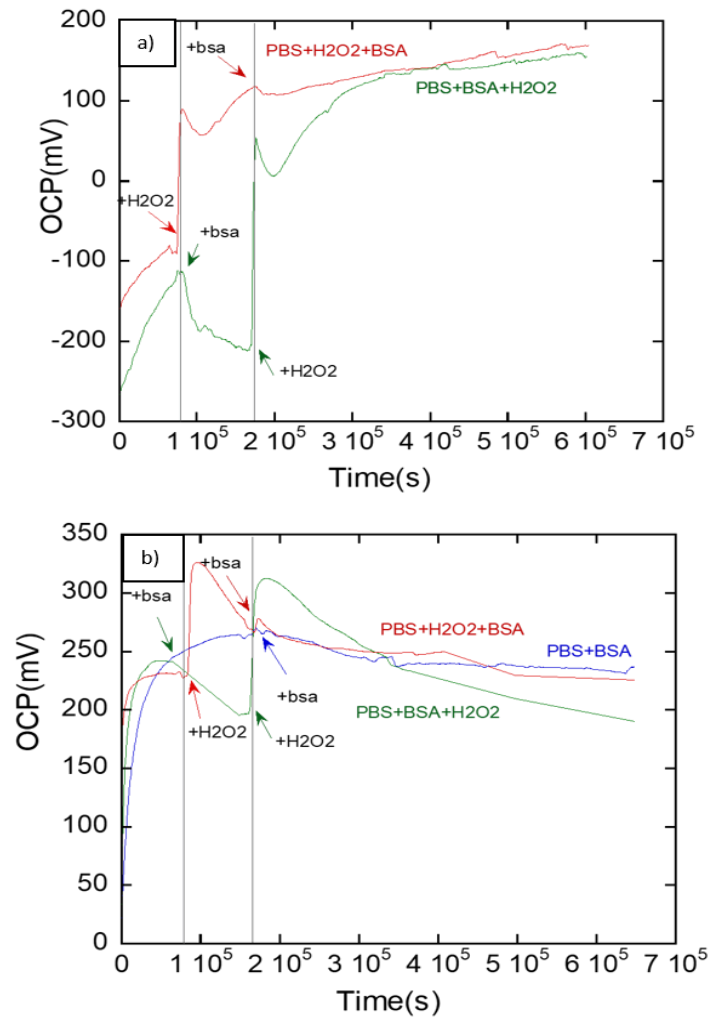


Figure 6.7 OCP as a function of time for (a) Ti6Al4V_MP and (b) Ti6Al4V_Treated_Ag in different physiological solutions: PBS with addition of H₂O₂ and albumin or just albumin as indicated by the arrows, at 37 °C.

- Figure 6.7a shows the OCP as a function of time for Ti6Al4V_MP in two different solutions (PBS+BSA+H₂O₂ and PBS+H₂O₂+BSA). The OCP starts with a low value (-300 mV), increasing to more positive values with time, reaching the stable value of OCP.

Generally, the OCP increases in the presence of H₂O₂ and decreases after the addition of albumin. The OCP of both samples, in the presence of mixed solutions of H₂O₂ and albumin, after 2×10^5 s (about 56 hours), tend to reach the same value.

When peroxide is added, in both cases the potential increases rapidly, reaches a maximum peak, decreases, and increases again.

H₂O₂ has an important role in the solution, as it introduces an high amount of oxidant in the solution which increases the cathodic reaction, due to the reduction reaction of H₂O₂, which for a stable anodic rate consequently increases the OCP.

Once the oxidant has accumulated on the interface, the surface of the titanium begins to react with it (known as complexation reactions [8] between H₂O₂ and TiO₂), which increases the anodic reactions due to destabilization of the oxide film, consequently decreasing the OCP. In fact, H₂O₂ has the effect of increasing the oxidation of the metal surface, forming a TiOOH complex. An alternative explanation for the decrease of OCP after the initial increase could be a reduced amount of H₂O₂ in solution.

- Figure 6.7b shows the OCP as a function of time for Ti6Al4V_Treated_Ag in three different solutions (PBS+BSA, PBS+BSA+H₂O₂ and PBS+H₂O₂+BSA). The OCP starts at a higher value than for the mirror-

polished sample (30 mV), since the surface has a thick layer of oxide produced by the treatment which ensures a smaller anodic area. Also in this case, when peroxide is added, the potential increases rapidly, reaches a maximum peak and decreases.

6.1.4.2. EIS Test

EIS Model

Once the OCP was finished, for some of the samples (*Table 5.5*) EIS tests were carried out. To perform a correct data analysis, an electric model was made, starting from the surface structure of the samples (view through the cross section, Figure 6.8).

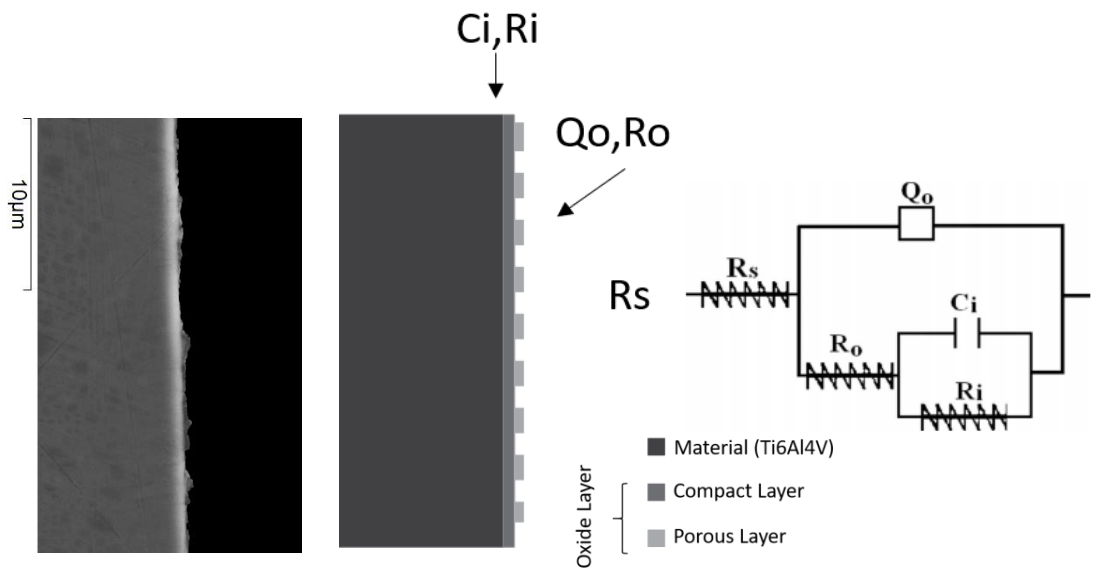


Figure 6.8 Model for EIS of Ti6Al4V_MP after PBS+BSA+H2O2 exposure, cross section (x5000), physical model and relative circuit electric model

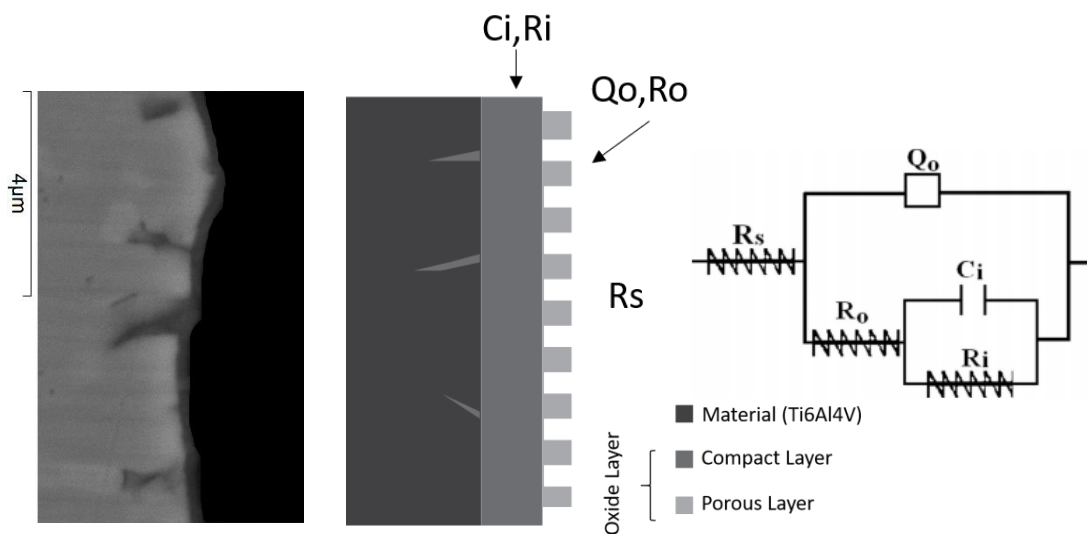


Figure 6.9 Model for EIS of Ti6Al4V_Treated after PBS+BSA+H2O2 exposure, cross section (x15000), physical model and relative circuit electric model

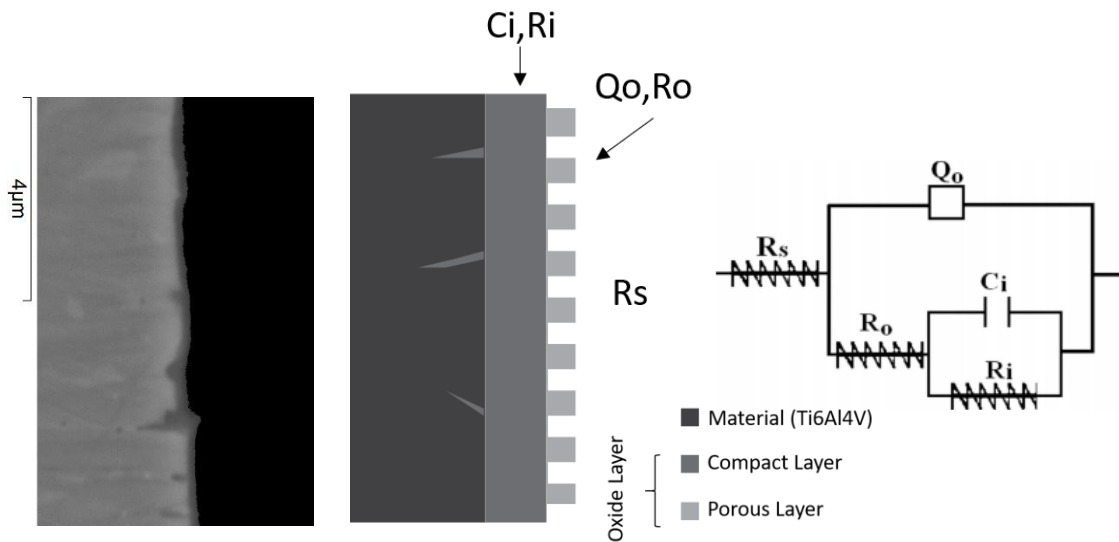


Figure 6.10 Model for EIS of Ti6Al4V_Treated_Ag after PBS+BSA+H2O2 exposure, cross section (x15000), physical model and relative circuit electric model

Equivalent circuits to fit EIS experimental data:

R_s is the resistance of the electrolyte, R_o and R_i represent the additional resistances of the outer porous layer and resistance of the inner and compact TiO_2 layer, respectively, C_i is the interfacial capacitance of the inner layer under the porous structure, Q_o is the constant phase element (CPE) of the entire oxide layer [2].

For the three different samples, a similar electric model was chosen, which respects the double model layer, inspired by the cross-section images of SEM, Figs. 6.8-6.10.

The main difference between the three models is the thickness of the two superficial layers, which are obviously thinner and less compact for the mirror-polished sample, which corresponds therefore to a lower value of C_i , R_i and R_o .

EIS Results

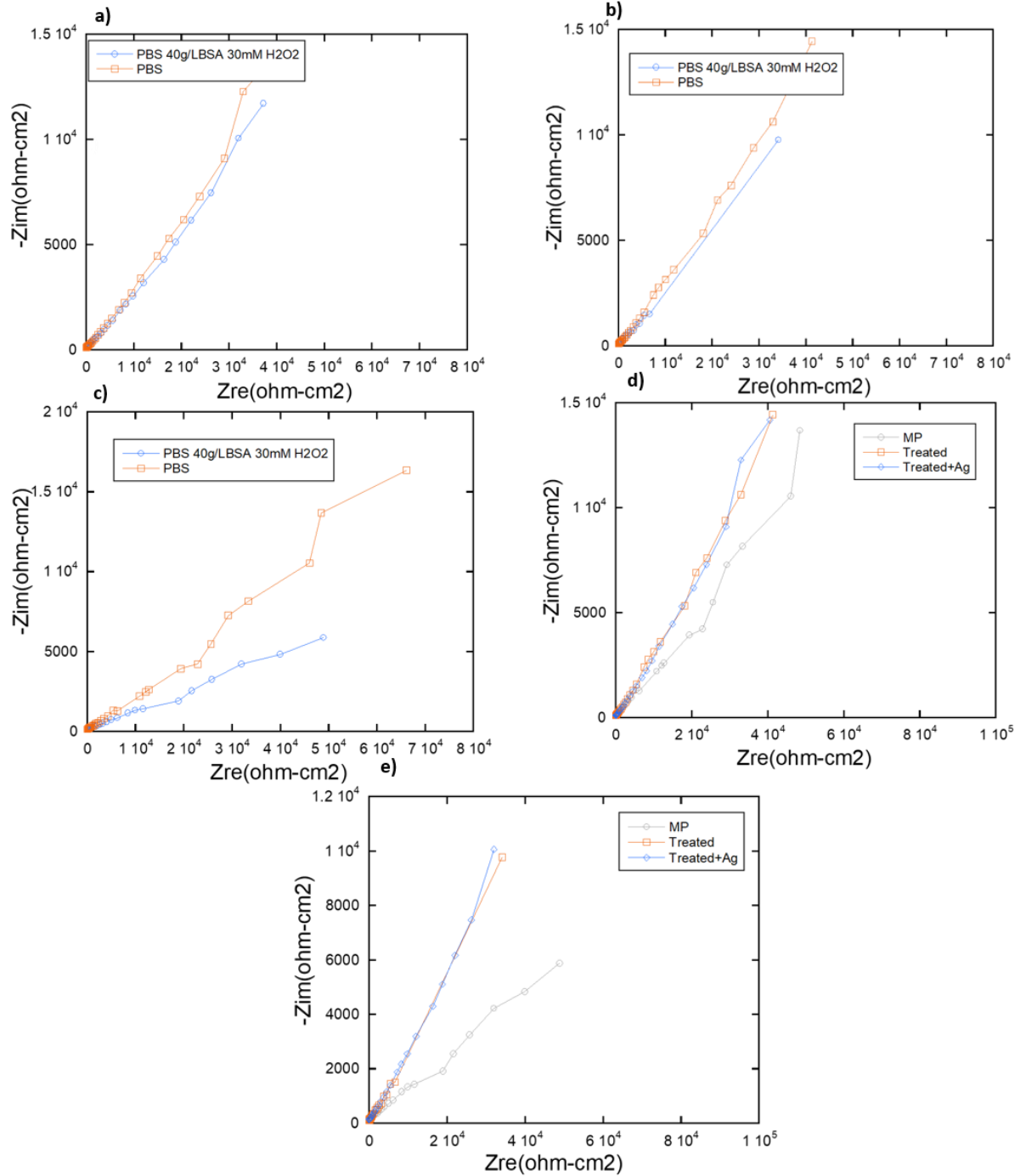


Figure 6.11 Nyquist plot for EIS response for (a) Ti6Al4V_MP (b) Ti6Al4V_Treated (c) Ti6Al4V_Treated_Ag, in two different solutions (PBS, PBS+BSA+H₂O₂) and for Ti6Al4V_MP, Ti6Al4V_Treated and Ti6Al4V_Treated_Ag immersed in (d) PBS and (e) PBS+BSA+H₂O₂, everything at 37 °C.

Figure 6.11a shows the Nyquist plot (Z_{re} , $-Z_{im}$) for mirror-polished samples in two different solutions, the less and the more aggressive. As expected, the sample immersed in PBS+BSA+H₂O₂, which is the more aggressive solution, has a lower resistance since the real part of the impedance (diameter of semicircle in Nyquist plot) decreased with the addition of BSA and H₂O₂ [1]. The same behaviour is presented for the other two samples (Ti6Al4V_Treated and Ti6Al4V_Treated_Ag, Figures 6.11b and 6.11c, respectively), even if the difference of resistance between PBS and PBS+BSA+H₂O₂ is less marked for the treated samples, as the layer of oxide is already thick and porous.

Figure 6.11d shows different samples in the same solution (PBS). It's clear, as expected, that the two treated samples (Ti6Al4V_Treated and Ti6Al4V_Treated_Ag) have a higher resistance, since they have a thick and porous layer given by the treatment, even if there is no remarkable difference between them, which means that the chosen frequency range is not suitable for detecting any difference in resistance of those two samples. The same trend was seen for the other solution (PBS+BSA+H₂O₂, Figure 6.11e).

6.1.4.3. Potentiodynamic Test

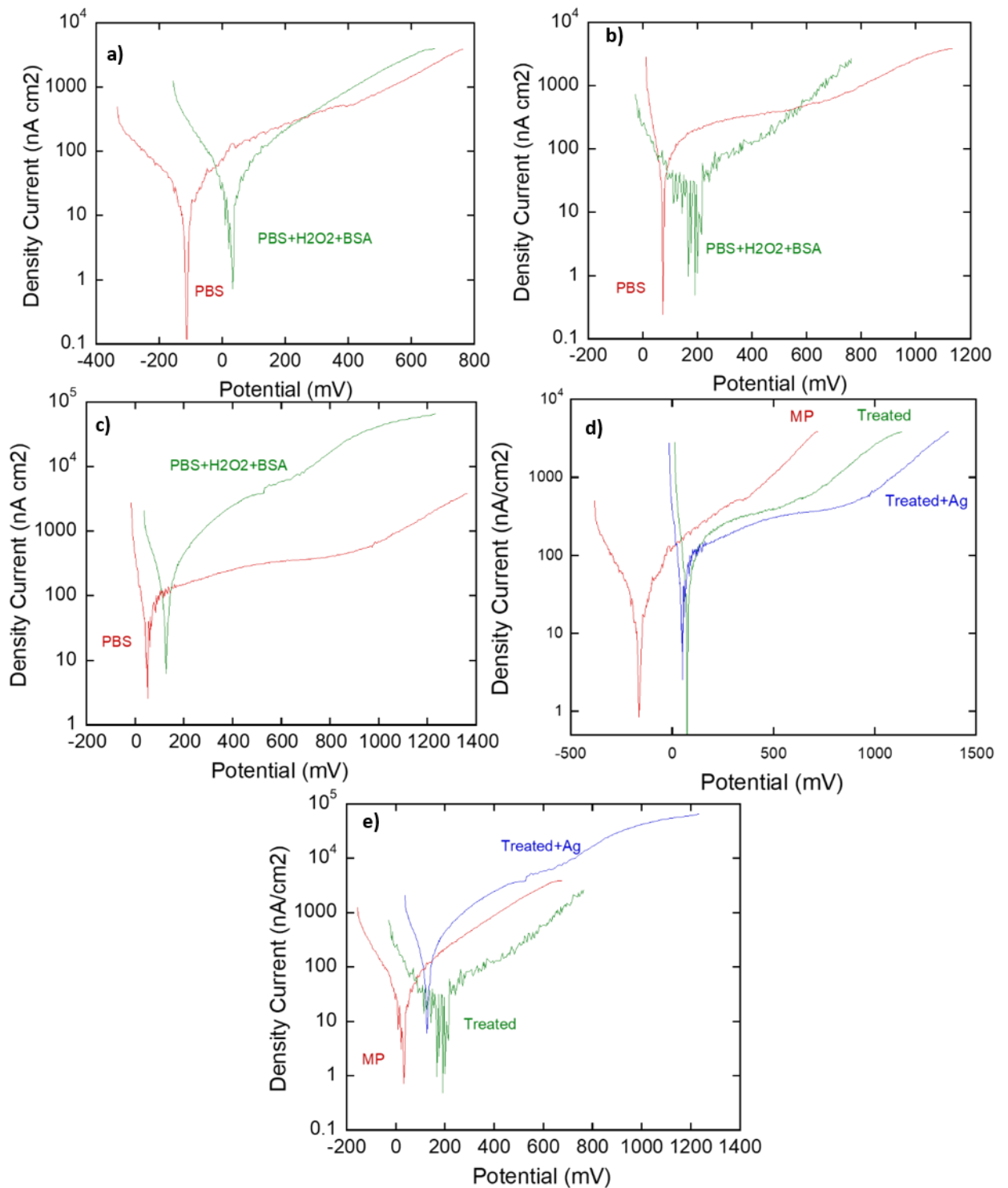


Figure 6.12 Potentiodynamic anodic polarization for (a) Ti6Al4V_MP (b) Ti6Al4V_Treated (c) Ti6Al4V_Treated_Ag, in two different solutions (PBS, PBS+BSA+H2O2) and for Ti6Al4V_MP, Ti6Al4V_Treated and Ti6Al4V_Treated_Ag immersed in (d) PBS and (e) PBS+BSA+H2O2, everything at 37 °C.

Figure 6.12a shows the polarization scan for mirror-polished samples (Ti6Al4V_MP) in two different solutions, the less and the more aggressive. For the mirror-polished alloy in PBS, the curve is characterized by a low value of E_{corr} (~ -200 mV), with a plateau from ~ 0 mV to $\sim +400$ mV followed by a slight increase, reaching probably the passive plateau, which could correspond to the structure composed by two layers. Upon adding BSA and H_2O_2 in the solution, significant differences in the polarization characteristics are observed: a shift of the E_{corr} towards more positive potential values and an increase in the anodic reaction rate above 300 mV, specifically, in agreement with a lower resistance found with EIS. The treated sample (Figure 6.12b) has a similar behaviour, in fact upon adding BSA and H_2O_2 in the solution, E_{corr} is higher, and there is an increase in anodic reaction rate above 600 mV, more positive than for the mirror-polished reference sample, as the curve in PBS solution presents a larger-ranged plateau at lower current values. The treated samples with silver (Figure 6.12c) present a different behaviour when BSA and H_2O_2 are added, the anodic current is increased significantly as compared to PBS, with a steady increase with increasing potential, reaching a plateau at relatively high values of current. Figure 6.12d shows different samples in the same solution (PBS). In comparison to the mirror-polished specimen, the two treated samples (Ti6Al4V_Treated and Ti6Al4V_Treated_Ag) have a positive shift in the value of E_{corr} and a decreased anodic current, which means that on their surfaces there is a more stable passive film. This is confirmed also by the presence of a big plateau (passive range) in the two treated samples, between ~ 200 mV to $\sim +800$ mV. The general shift of the Tafel plot towards more positive potential values and a decrease in the anodic current indicates inhibition in the rate of dissolution process for the corroding-passivating surface oxide film [3]. The

electrochemical corrosion parameters (E_{corr} and i_{corr}) were evaluated from the polarization curves and presented in Table 6.4 and in Table 6.5. The samples with silver have a lower E_{corr} than the samples without silver with a slightly higher i_{corr} , which suggests, as expected, that the passive layer on the surface is thinner and less compact as compared to the treated sample without silver. The different characteristic of the treated sample with silver in the most aggressive solution with BSA and H_2O_2 (Figure 6.12) suggests galvanic or other effects induced by silver, maybe hindering repassivation (as compared to treated samples or mirror-polished titanium alloy). The current is 4-fold higher as compared to the other samples.

Table 6.4 Corrosion parameters evaluated with Tafel method, for PBS solution

	E_{corr} (mV)	i_{corr} (A/cm ²)
MP	-178	5.48E-08
Treated	116	3.75E-08
Treated+Ag	96	4.10E-08

Table 6.4 Corrosion parameters evaluated with Tafel method, for PBS+BSA+H₂O₂ solution

	E_{corr} (mV)	i_{corr} (A/cm ²)
MP	37	6.44E-08
Treated	170	3.25E-08
Treated+Ag	120	1.94E-07

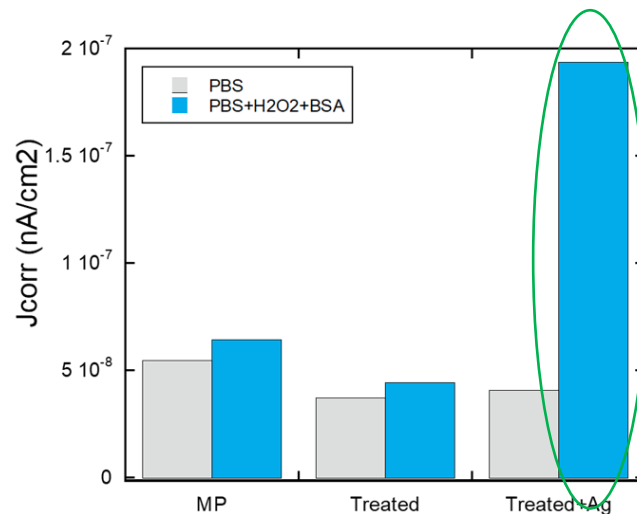


Figure 6.13 Current density of corrosion (i_{corr}) for all samples (Ti6Al4V_MP, Ti6Al4V_Treated, Ti6Al4V_Treated_Ag), in different solutions

6.1.5. Metal Release

After the electrochemical test, the released and non-precipitated amounts of titanium, aluminum, vanadium and silver in the different solutions were investigated by means of graphite furnace atomic absorption spectroscopy.

Before this project, another project which investigated the ionic and nanoparticle release mechanism of similar samples was made, immersing the samples in different solutions, not considering the electrochemical part, with the purpose to lay the foundation for understanding the corrosion behaviour that is analysed with this thesis. This data is considered here for comparative reasons as well.

Therefore, metal release from mirror-polished samples, treated samples and treated samples with silver, from Padoan's thesis [6] are also reported.

The results (*Figure 6.14*) are outcomes from an exposure in PBS + 30mM H₂O₂ + 40g/L BSA for 2 weeks, instead of 1 week, without the electrochemical test,

conditions that partially differ from this study. However, they can still be important for comparison and to check how the potentiodynamic test can affect the metal release.

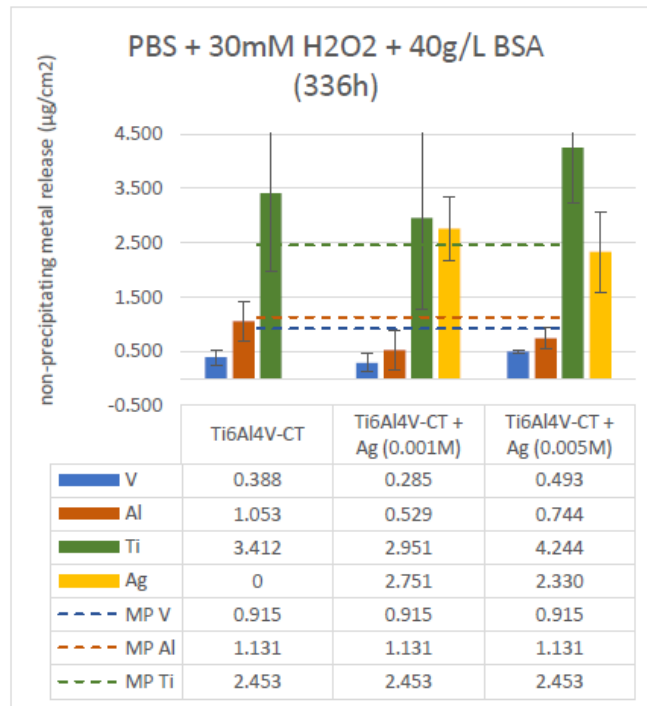


Figure 6.14 AAS analysis of solutions in contact with Ti6Al4V samples in the previous work, used to compare the results of this project. Ti6Al4V-CT corresponds to Ti6Al4V_Treated, Ti6Al4V-CT+Ag (0.001M) corresponds to Ti6Al4V_Treated_Ag, Ti6Al4V-CT+Ag(0.005M) it is not to be taken into consideration, since the concentration of silver is different from that of the samples used here. [6]

For comparison, metal release from an abraded Ti6Al4V alloy from Hedberg et al. [7] are also reported. That study investigated, as a function of different amounts of hydrogen peroxide and bovine serum albumin, the mechanism of the synergistic combination on the metal release. (Figure 6.15)

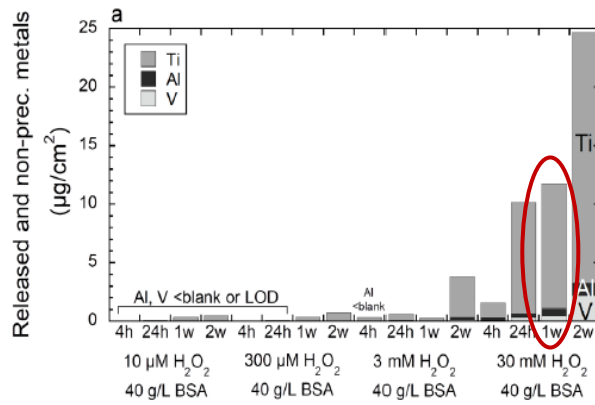


Figure 6.15. Metal release from Ti6Al4V alloy dependent on H₂O₂ and BSA amount [7]

For comparison to this study, only the encircled part can be considered.

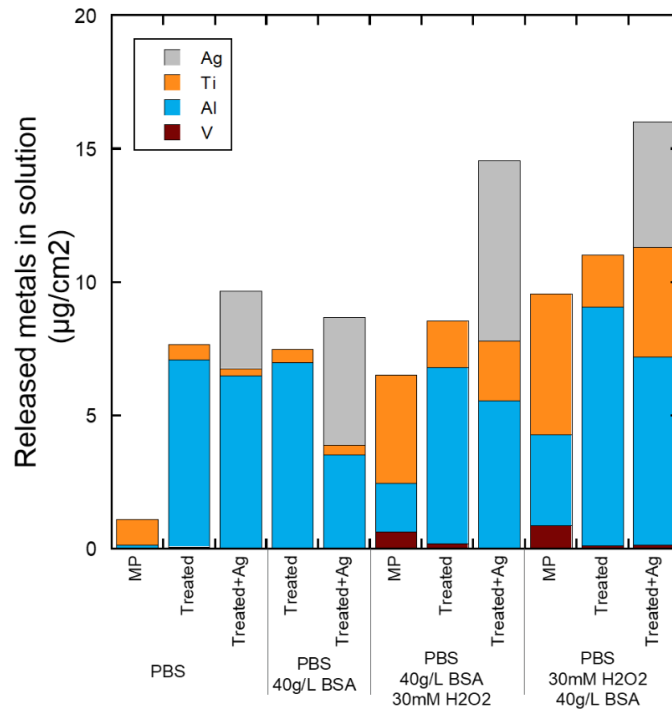


Figure 6.16 Metal release from Ti6Al4V_MP, Ti6Al4V_Treated, Ti6Al4V_Treated_Ag in different solutions.

Figure 6.16 shows the metal release results of this project. As expected, in all cases, the release is higher when there is the combination of BSA and H₂O₂. It also seems that there is an even higher release when the H₂O₂ is added first.

The mirror-polished sample has unexpected values of release, as the ratio between the various elements didn't agree with the ratio found in previous work (*Figure 6.15*). In fact, the release of aluminium is higher and the release of titanium lower than in immersion tests of one day previously abraded samples without any applied potential (Al release is four times higher than in Hedberg et al. 2019 [7]). Regarding the treated samples, the amount released of titanium and vanadium is lower than for the mirror-polished alloy, while the amount released of aluminium is undoubtedly higher which results in a higher total release of elements. This indicates that the measured metals in solution do not totally reflect the electrochemically dissolved amounts of metals, as from the electrochemical tests (*Table 6.4*) a lower total release of elements would be expected from the treated samples. It has previously been shown that electrochemical dissolution is only a part of the metal release from TiAlV alloy [7]. This is particularly important for Al, which binds to albumin and chloride ions [7] and could for the same reason be prevented from precipitation, as would be expected from the calculated Pourbaix diagram in pure water (*Figure 6.17*). Titanium is probably underestimated in all solution, as it is not stable in PBS (*Figure 6.17*) and due to the electrochemical cell setup probably lost to the sample and cell walls as precipitates. The silver follows the same trend than the other elements, as it is more released upon adding H₂O₂ and BSA even if the amount is relatively high (two times higher than in Padoan's work) (*Figure 6.14*) but this could be due to the unexpected size and distribution of silver particles or the potentiodynamic polarization. Silver ions could be stable in PBS after

the potentiodynamic polarization and in the presence of hydrogen peroxide, see *Figure 6.17*. Vanadium is stable in PBS, see *Figure 6.17*, and therefore probably detected as closely as possible to the released amount. That it is released to a significantly lower extent from the treated samples is expected, since vanadium is the first element released from the surface oxide [7] and therefore probably already depleted during the surface treatment (it was also not found in the EDS analysis). It is possible to see from the comparison between the previous and the current work that the application of the high oxidation potential during the potentiodynamic polarization results in a higher total released amount of metals in solution.

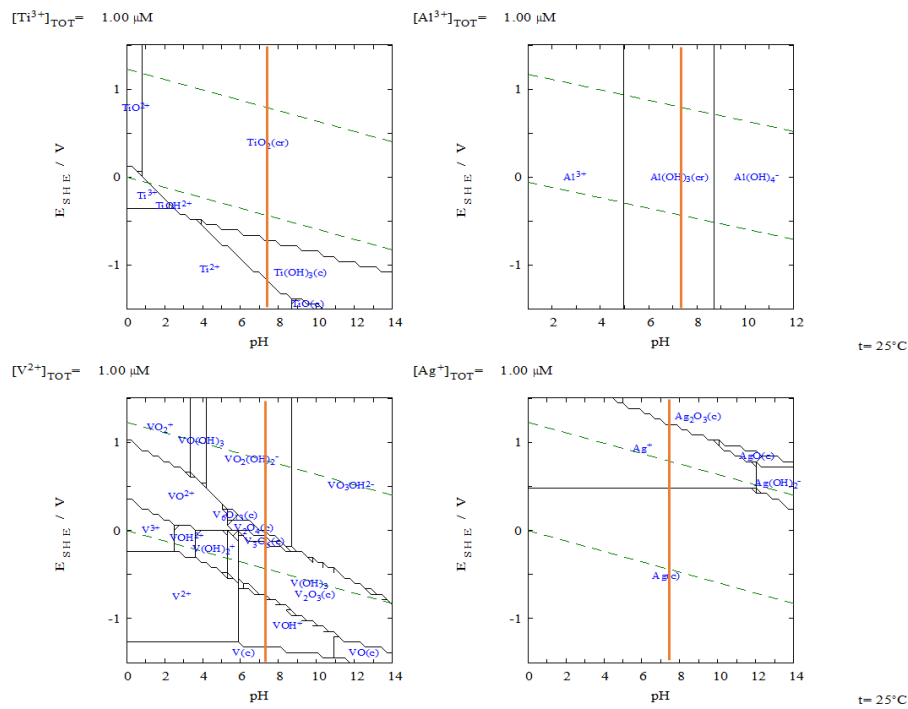


Figure 6.17. Calculated Pourbaix (pH-potential) diagrams with the Hydra/Medusa software (<https://www.kth.se/che/medusa/downloads-1.386254>) indicating the pH of PBS (pH 7.3). These predominance diagrams show that Ti and Al are not stable in solution and would precipitate. Al might be stabilized in solution by binding to chloride anions or albumin though [7] (not included in these equilibrium diagrams in water). Ag can be in the ionic form if the equilibrium potential is high enough (by hydrogen peroxide or applied potential), and vanadium is soluble.

Chapter 7

7. Conclusions

This thesis aimed on studying the corrosion and release behaviour of samples of the biomedical alloy Ti6Al4V functionalized with nanoparticles of antimicrobial silver and optimized for osseointegration. This was accomplished by surface treatments at Politecnico di Torino's laboratory and a multi-analytical approach at KTH Royal Institute of Technology including several electrochemical, spectroscopic and surface analytical methods. The surface treatment consisted of an acid etching followed by a controlled oxidation to make the surface chemically and topographically suitable for cell adhesion and for osseointegration. Insertion of AgNO₃ solution with stabilizing and reducing agents during controlled oxidation aimed on incorporated and surface-attached silver nanoparticles for an antibacterial effect. To mimic the physiological environment in the human body during infection, samples were exposed to a physiological solutions based on phosphate buffered saline (PBS) with varying hydrogen peroxide (H₂O₂) and bovine serum albumin (BSA) concentrations at a constant temperature of 37 °C. The following main conclusions were drawn:

- Surface characterization showed that functionalization of silver was heterogeneous and uneven, resulting in micron-sized agglomerates, probably due to a problem with stabilizing agents. The surface also revealed cavities, in which aluminium was absent, probably due to the process of acid etching with hydrofluoric acid during treatment. Treatments resulted in micrometer-thick, rough and porous oxides rich of titanium, ideal for osseointegration. Colour analysis showed some differences among

treatments with and without silver nanoparticles.

- Treated Ti6Al4V had a higher corrosion resistance than mirror-polished Ti6Al4V not treated. The presence of silver nanoparticles detrimentally affected the corrosion behaviour only in the most aggressive physiologically simulated environments (PBS with 40 g/L BSA and 30 mM H₂O₂), but not in PBS.
- Metal release was smallest in PBS, greater in PBS+40 g/L BSA, and largest in PBS+40 g/L BSA +30 mM H₂O₂. However, the influence of the solution was greater for the mirror-polished sample than for the treated samples, probably due to previous oxidation and passivation. Vanadium was only released from the mirror-polished alloy, due to a depletion of vanadium in the oxide during the treatment for the treated samples. Silver was released to a higher extent than titanium, which is partially explained by solution chemistry (no precipitation) and was also visible in post-exposure scanning electron microscopy analysis. No silver was found on the surface after exposure. Titanium release was probably underestimated due to precipitation at that pH. Aluminium release was markedly higher for the treated samples as compared to the mirror-polished sample, probably due to a larger surface oxide surface and interactions with BSA and chlorides.

References:

- [1] Zhang Yue, Addison Owen, Yu Fei, Rincon Troconis Brendy, R. Scully, John, Davenport, Alison.
“Time-dependent Enhanced Corrosion of Ti6Al4V in the Presence of H₂O₂ and Albumin” Scientific Reports, 2018.
- [2] Xiangmei Liu¹, Shuilin Wu^{1, 2}, Kelvin W. K. Yeung³, C.Y. Chung², Paul K Chu².
“Surface Coloration and Electrochemical Impedance Spectroscopy Characterization of Oxygen Plasma Implanted Orthopaedic Titanium Alloys”
Int. J. Electrochem. Sci., 7 (2012) 6638 – 6653
- [3] F. El-Taib Heakal* , Kh.A. Awad
“Electrochemical Corrosion and Passivation Behavior of Titanium and Its Ti-6Al-4V Alloy in Low and Highly Concentrated HBr Solutions”
Int. J. Electrochem. Sci., 6 (2011) 6483 – 6502
- [4] Fei Yu
“Corrosion of Titanium for Biomedical applications”
Thesis, University of Birmingham, March 2015
- [5] Yu, F., Addison, O. & Davenport, A. J. *“A synergistic effect of albumin and H₂O₂ accelerates corrosion of Ti6Al4V”*. Acta Biomater. 26, 355–365 (2015).
- [6] G. Padoan
“Preparation and characterization of Ti-6Al-4V surfaces functionalized with silver for antibacterial purposes: study of ionic and nanoparticles release mechanism”
April, 2018
- [7] Hedberg, Y. S., Žnidaršič, M., Herting, G., Milošev, I. & Odnevall Wallinder, I. J. Biomed. Mater. Res. B, 107 (2019) 858-867, *“Mechanistic insight in the synergistic dissolution of TiAl6V4 by albumin and hydrogen peroxide – importance of albumin-aluminium binding.”*
- [8] Pan, D. Thierry, C. Leygraf,
“Hydrogen peroxide toward enhanced oxide growth on titanium in PBS solution: blue coloration and clinical relevance”, J. Biomed. Mater. Res., 30 (1996) 393-402.